AFFDL-TM-73-163-FXG

AIR FORCE FLIGHT DYNAMICS LABORATORY
DIRECTOR OF SCIENCE & TECHNOLOGY
AIR FORCE SYSTEMS COMMAND
WRIGHT-PATTERSON AIR FORCE BASE OHIO

RESULTS OF CALIBRATION TESTS CONDUCTED IN THE AFFDL 2 FOOT ELECTROGASDYNAMIC FACILITY

Max E. Hillsamer

November 1973

Project Number 1366
Task Number 136603

Approved for public release; distribution unlimited

High Speed Aero Performance Branch
Flight Mechanics Division
Air Force Flight Dynamics Laboratory

~~AFFDL-TM-73-163-FXG~~
AFFDL-TM-73-163-FXG

RESULTS OF CALIBRATION TESTS CONDUCTED IN THE AFFDL 2 FOOT ELECTROGASDYNAMIC FACILITY

Max E. Hillsamer

November 1973

Project Number 1366
Task Number 136603

High Speed Aero Performance Branch
Flight Mechanics Division
Air Force Flight Dynamics Laboratory

FOREWORD

This technical memorandum was prepared by the Aerothermodynamics Group of the High Speed Aero Performance Branch, Flight Mechanics Division, Air Force Flight Dynamics Laboratory under Task Nr. 136603 "Aerodynamic Heating to Military Vehicles" of Project Nr. 1366 "Aero-performance and Aeroheating Technology."

Instrumentation and facility operations were conducted by personnel from Experimental Engineering Branch (AFFDL/FXN), and the facility operator for the entire test period was Mr. J. A. Funderburg of the High Speed Aero Performance Branch (AFFDL/FXG). The author gratefully acknowledges their cooperative assistance.

This technical memorandum has been reviewed and is approved.

PHILIP P. ANTONATOS
Director
Flight Mechanics Division

ABSTRACT

Calibration tests have been conducted in the Two Foot Electrogasdynamics Facility (2 Ft EGF) to determine test section core size and flow parameters. Results contained in this report cover a 5 year period and consist of data obtained using the 7.19 and 19.36 inch exit diameter conical nozzles. Measured test section parameters are local mass flux, impact pressure and heat flux, with local freestream velocities and densities and stagnation enthalpies being calculated.

Results shown indicate fluctuations in measured parameters and the necessity for further developmental work to enhance the usefulness of the facility as an aerodynamic research tool. Calibration runs are necessary at each required operating condition for any test program in the facility and must be conducted in conjunction with the test program. Parameters presented in this report are useful for obtaining an estimate of flow conditions expected for future test planning.

TABLE OF CONTENTS

TABLES

ILLUSTRATIONS

LIST OF SYMBOLS

d	Diameter, inches
E	Voltage, volts
FM_{1-5}	Water flow rates, gpm
H	Enthalpy, BTU/lbm
I	Current, amperes
K	Orifice discharge coefficient, dimensionless
$\dot{M}$	Air flow rate, lb/sec
P	Pressure, psia or MM Hg (specified)
$\dot{q}$	Heat transfer rate or heat flux, BTU/ft^2-sec
R	Radius, inches
T	Temperature, deg R
U	Velocity, ft/sec
Δ	Differential measurement
α	Diffuser contraction included angle
ρ	Density, lb/ft^3
Subscripts	
DT	Diffuser throat
DI	Diffuser inlet
HB	Heat Balance
IN	Input to arc heater
Int	Integrated from local measurements across jet face.
Loss	Arc heater losses

LIST OF SYMBOLS (CONT'D)

LU	Upstream air line measurements
NE	Nozzle exit
NS	Nozzle static
0	Stagnation or total conditions
T2	Local impact measurement
TS	Test section
w	Wall conditions
∞	Freestream conditions

I. INTRODUCTION

The Two-Foot Electrogasdynamics Facility (2 Ft EGF) is an arc heated, hypersonic wind tunnel operated by the High Speed Aero Performance Branch, Flight Mechanics Division of the Air Force Flight Dynamics Laboratory (AFFDL). The 2 Ft EGF serves as a high enthalpy research tool with the advantage of economy and flexibility of operation.

The 2 Ft EGF is capable of Mach 6 to 12 operation at bulk enthalpy levels to 7500 BTU/lbm. Arc heaters are tubular coaxial electrode type operating on a maximum 4 megawatts rectified D.C. power with high pressure air as the test gas. The conical nozzles used have 7.19 or 19.36 inch exit diameters, and a 9.5 inch exit diameter Mach 10 contoured nozzle is available. An open jet test section is used, and the replaceable diffusers are sized to match the available nozzles.

Beachler (Reference 1) presents a brief history of the facility along with results of test section calibration runs with the 7.19 and 19.36 inch nozzle systems before 1968. Zonars (Reference 2) presents calibration results obtained with the 9.5 inch contoured nozzle at 3 test conditions. Further calibration data with the conical nozzles is presented in Reference 3. Because of the infinite number of test conditions obtainable by varying stagnation pressure and power input to the arc heater, only certain selected conditions were tested and documented in References 1-3.

In order to eliminate a great number of variables and still provide useful operating points for tests, calibration runs since 1968 have concentrated on obtaining repeatable results at three widely separated test

conditions with the conical nozzles. The conditions chosen were high stagnation enthalpy and low stagnation pressure, high pressure and low enthalpy, and an intermediate pressure/enthalpy point. The conditions, described in Section IVA, were not maximum or minimum operating limits of the arc heaters and other associated equipment, but were chosen to provide a useful test range with optimum equipment life.

Results presented in this report are from 7.19 and 19.36 inch conical nozzle calibration tests using a standard 0.4375 inch diameter nozzle throat and two arc heaters of different operating characteristics. Flow diagnostic probes used consisted of a combination mass flux - impact pressure probe and a steady state calorimeter. Local stagnation enthalpy, freestream velocity and freestream density were calculated from parameters measured by the diagnostic probes.

II. FACILITY DESCRIPTION

The 2 Ft EGF consists of a heat source provided by a coaxial electrode arc air heater and a test leg which includes the nozzle system, test cabin, diffuser system and heat exchanger. The high pressure air supply, 4 megawatt power supply and vacuum system complete the facility. A schematic is presented in Figure 1.

The arc heaters used in the calibration tests were designated N-4000 and N-4001 heaters and were designed by Linde Div., Union Carbide Corp. and modified in-house. The N-4000 arc heater is designed for relatively high pressure and moderate enthalpy operation while the N-4001 arc heater is designed for moderate pressure/high enthalpy operation. Cutaway views of the arc heaters are shown in Figures 2 and 3.

The test cabin is of the open jet type with free jet length from 14.50 to 28.50 inches, determined by the nozzle/diffuser combination used. The model injection system, located in the bottom of the test cabin, is capable of 14.5 inches of axial traverse or model pitch angles from -5 to +45 deg and 360 deg of roll. In addition to the model injection system, two struts are injected across the nozzle centerline from 37.5 deg above the horizontal center plane of the test section. The side struts are used for flow diagnostic probe insertions and provide the capability of making flow calibration checks during a test run. Each system can be injected manually, swept to a designated point in the flow and out, or stepped in and/or out of the flow in 8 increments. Figure 4 shows a schematic of the test cabin with nozzle/diffuser systems outlined.

The nozzle/diffuser combinations used during the calibrations runs are presented in the table of Figure 5. Both nozzles were 15 deg conical nozzles with 0.4375 inch diameter throats. The nozzle throat sections are an integral part of the arc heater front electrode thereby utilizing the front electrode water cooling system. The expansion section of the nozzles was cooled by a separate low pressure water source.

The diffuser used with the 7.19 inch diameter nozzle was the same as reported in Reference 1 and shown as Configuration I in Figure 5. During calibration tests prior to 1970, a 21 inch throat diameter uncooled diffuser, listed as Configuration II in Figure 5, was used with the 19.36 inch nozzle. Modifications to the facility in 1970 included the installation of a water-cooled diffuser with a throat diameter of 22 inches and a length of 327.5 inches. This diffuser is shown in Configuration III of Figure 5.

The air/water heat exchanger, composed of 12 rows of 1 inch dia. copper tubes is located at the outlet end of the diffuser system. In order to accommodate the increased length of diffuser throat from Configuration II to III, all tubes in the heat exchanger casing were moved downstream as far as practical, and the diffuser outlet was extended into the heat exchanger casing. Thermocouples located in the heat exchanger tubes indicated that the reconfigured heat exchanger effectively cooled the hot test gases to less than 100°F before the gases entered the vacuum system.

The high pressure air supply system consists of 9 high pressure air vessels with a total capacity of 548 cubic feet. The vessels were charged to 2500 psia by a 7 stage converted nitrogen compressor capable of supplying 2 lb/sec of dry air at 2500 psia. A metering orifice, throttling valve, high pressure regulator and isolation valves complete the system.

The vacuum system consists of a 66,000 cubic foot vacuum sphere and 19 mechanical pumps. The vacuum system is connected to the test leg in the arrangement shown in Figure 1 and is capable of evacuating the test leg to less than 0.1 Torr for initial startup. During a test run all pumps are on and the vacuum sphere is connected to the test leg to produce maximum operating times.

The direct current power supply used in the 2Ft EGF is composed of 4 full wave silicon diode rectifier units, each rated at 500 KW. The units can be connected in series, parallel or series/parallel arrangements and operated at 100% overload for up to 5 minutes to produce a maximum available power of 4 MW. The operating time for the power supplies is limited primarily by transformer temperature.

Three separate cooling water systems are used to protect 2 Ft EGF equipment from overheating. Cooling water to the arc heaters is supplied at 500 psig from a closed circuit demineralized system capable of delivering 300 gpm. The nozzle effuser section, diffuser, power supplies, test cabin, and air/water heate exchanger are cooled by a 125 psig coolant system capable of supplying 1200 gpm of softened water. A seven channel chemically softened water system, delivering 16 gpm at 600 psia, is used for cooling struts and probes in the test section.

III. INSTRUMENTATION AND DATA COLLECTION

Each component of the facility was instrumented as fully as possible to provide accurate pressure, temperature and flow rate records where required. While not all of the measured parameters are used in determining aerodynamic flow characteristics of the facility, many of the measurements are necessary to aid in detecting possible component failures and to be used as inputs to the facility safety interlock system. Reference 4 describes the instrumentation for each component of the facility, and Table I presents a brief description of each instrumentation item used to obtain results presented in this report. Ranges and accuracies are given where applicable and known.

A safety interlock system is utilized in the 2 Ft EGF which permits safe automatic shutdown of the facility if any one of the critical components fails in any way. A time resolved system of annunciators located at the operator's console aids in determining the cause and location of a component failure during a test run. Reference 1 contains a complete description of the safety interlock system.

A combination mass flux-impact pressure probe and two different types of hemispherical steady state calorimeters were used to measure flow properties in the test section. The mass flux-impact pressure probe, fully described in Reference 5, is an aspirating type probe with an accurately measured sharp edged inlet. When used to measure mass flux, the gas sample is passed through a low density flow transducer for measurement and into a combination vacuum pump and storage system. The pressure differential through the mass flux measuring system is sufficient to assure swallowing

of the bow shock at the probe tip. A valve upstream of the low density flow transducer allows closing of the mass flux measuring system when the probe is used to measure impact pressure. The response time of the system requires approximately 5 seconds to obtain a stabilized mass flux measurement and about 3 seconds for an impact pressure measurement.

The first steady state calorimeter used contained a 0.530 inch diameter copper slug faired into the 1.0 in. diameter probe tip. The slug is insulated from the probe body, and a spiral groove is machined in the back surface. Heat is removed from the known area of the probe tip by passing cooling water at high velocity through the spiral groove. Inlet and outlet temperature and flow rate of the cooling water are measured to determine heat input to the slug. This probe is capable of measuring heat transfer rates from 100 to 420 BTU/ft^2-sec with an accuracy of $\pm$10% of the measured reading. The response time of the system requires 8-10 seconds to obtain stabilized measurements of parameters to calculate heat flux. A total time of approximately 90 seconds is required to complete an eight step survey of the test core. More complete details of this probe are presented in Reference 5.

A high response steady state calorimeter has been used to measure heat flux in the facility. The high response probe has the same dimensions as the standard calorimeter, but a Gardon type heat flux sensor is installed in the probe tip instead of the swirl insert. The Gardon sensor, shown in Figure 6, consists of a disk of constantan foil exposed to the airstream and connected to a copper heat sink. The sensor is precalibrated to produce a millivolt signal which converts directly to BTU/ft^2-sec without the necessity of measuring water flow rates and inlet and outlet temperatures.

Approximately 3 seconds is required to obtain a heat flux measurement at each probe position. Heat transfer rates to 500 BTU/ft^2-sec can be measured by the high response calorimeter with an accuracy of $\pm$10 percent.

Various types of amplifiers, filters and reference junctions are used to condition the signals obtained from the facility instrumentation. Figure 7 is a schematic of the data processing system showing the input parameters, signal conditioning equipment, recording and monitoring apparatus. Strip chart recorders, visicorders and meters are available for on-line monitoring of facility parameters during a test run. A 200 channel data logger, equipped with a paper tape punch is used to record data during calibration of the instruments. The data logger is too slow, however, to be used during tests.

Analog signals from the facility are passed through a 160 channel analog-to-digital converter and stored on magnetic tape at the rate of 57 scans per second. Final data reduction is accomplished on a CDC-160A computer within 30 minutes after a test run.

IV. TEST DESCRIPTION

A. Test Conditions - The original concept of this study was to obtain calibration data at many different operating conditions. Because of the wide range of operating conditions possible in this facility it was decided to limit the study to three pressure/enthalpy levels and concentrate on obtaining several repeat runs at each operating level. One nozzle throat size, 0.4375 in. dia., was used, and stagnation conditions were chosen to provide a minimum, intermediate and maximum operating pressure with stable flow and no arc blow-out.

While early calibration runs were conducted at minimum pressure levels of 150 and 200 psia, the major part of this study has been conducted at pressure levels of 250, 350 and 500 psia, which represent more stable operating points, with respective arc current levels of 1800, 750 and 550 amps. Table II is a listing of valid calibration runs made in the 2 Ft EGF which have some flow parameters presented in this report. Conditions listed in Table II are average values for the entire test run. Table III presents a comparison of stagnation pressures, enthalpies and mass flows desired and average conditions achieved during the calibration tests.

B. Test Procedure - Immediately prior to each test run an air-off data point was recorded for use as initial zeros in data reduction. After flow had been established and stabilized in the test section, each flow diagnostic probe was injected to nozzle centerline in 8 steps starting just inside the nozzle edge. Approximately 15 scans (0.25 sec) of data were recorded at each step. A final air-off data point was recorded after tunnel shutdown to determine any zero shift of the instrumentation during the test run.

C. Data Reduction - Raw voltages on each channel were averaged for each test point, and data were reduced to parameter form through least squares curve fits from constants obtained from instrument calibrations. In most cases, a first order (straight line) curve fit was sufficient. Supply line pressure and stagnation pressure reduced zeros were set equal to atmospheric pressure, and various other pressure reduced zeros were set equal to test cabin static pressure in order to account for any instrumentation electronic shifts.

Bulk stagnation, or heat balance, enthalpy was calculated by subtracting measured heat losses in the arc heater/nozzle from the measured power input to the arc heater, or

$$H_{ONB} = H_{IN} - H_{LOSS} \tag{1}$$

$$H_{IN} = \frac{.9481\ EI}{1000\ \dot{M}}\ ,\ BTU/lbm \tag{2}$$

$$H_{Loss} = \frac{\Delta T_1 F_{M1} + \Delta T_2 F_{M2} + \Delta T_3 F_{M3} + \Delta T_4 F_{M4} + \Delta T_5 F_{M5}}{7.2\ \dot{M}}, \frac{BTU}{lb_m} \tag{3}$$

Locations of ΔT_i and F_{M_i} measurements are listed in Table I. Mass flow was calculated from the relation

$$\dot{M} = k\sqrt{\frac{(P_{LL})(\Delta P)}{T_{LL}}}\ ,\ lb/sec \tag{4}$$

where k = predetermined discharge coefficient

A relationship between heat flux, impact pressure and enthalpy was derived in Reference 7 as

$$\dot{q}_s = \lambda(\sqrt{2})^{t-1}\sqrt{\frac{P_{T_2}}{d_o}}(H_o - H_w)(10^{-6}) \tag{5}$$

Reference 7 has shown from a simplification of the Fay and Riddell relation (for Lewis Nr. = 1 and Prandtl Nr. = .71) that

$\lambda = 2.25$ and

$t = 1$ for blunt nose axisymmetric bodies

Therefore equation (5) can be written as

$$H_o = \frac{\dot{q}_2}{2.25}\sqrt{\frac{d_o}{P_{T_2}}}(10^6) + H_w \quad , \quad ft^2/sec^2$$

or

$$H_o = 17.77\,\dot{q}_2\sqrt{\frac{d_o}{P_{T_2}}} + H_w \quad , \quad BTU/lb_m \qquad (6)$$

where do = calorimeter diameter, inches

and Hw = residual enthalpy in the calorimeter, approximately 120 BTU/lbm

Measurements of local mass flux, $(\rho u)_\infty$, and impact pressure, P_{T_2} were used with an empirically determined factor of 0.94 to calculate velocity and density by modified Newtonian theory and

$$P_{T_2} = 0.94\,\rho_\infty u_\infty^2 \gg P_\infty \qquad (7)$$

where P_{T2} is in lb/ft^2, ρ_∞ is in $slugs/ft^3$ and u_∞ is in ft/sec. Rearranging and converting P_{T2} to MM Hg and ρ_∞ to lb/ft^3, equation (7) becomes

$$u_\infty = \frac{144g\,(.01934)\,P_{T_2}}{0.94\,(\rho u)_\infty} = \frac{85.6\,P_{T_2}}{(\rho u)_\infty}, \quad ft/sec \qquad (8)$$

Density (or more correctly, specific weight) is then calculated from the relation

$$\rho_\infty = \frac{(\rho u)_\infty}{u_\infty}, \quad lb/ft^3 \tag{9}$$

V. RESULTS

A. General - Data from a total of 114 test runs are presented in this report. Much of the data was obtained during operations for other test programs with various parameters not being measured. Most notable is the lack of mass flux profiles for the 500 psia condition with the 7.19 inch nozzle and the lack of heat flux profiles at all 7.19 inch nozzle conditions. Where possible each profile is the average obtained from several runs, and maximum and minimum valves are shown on the curves.

Variations in operating parameters are presented in Figures 8, 9, and 10. Each point on the figures is an average of several runs listed in Table II. Vertical lines on Figures 8 and 10 indicate maximum run-to-run deviations from average values at the stagnation pressures tested. The inability to set and repeat desired operating conditions from run to run is an inherent characteristic of this type of facility and the arc heaters used. During a test run the stagnation pressure and arc current are controlled, and arc voltage and mass flow are allowed to stabilize where they will. Voltage levels achieved depend on electrode condition and the development of arc attachment points in the arc heater. Measured parameters used to calculate heat balance enthalpy, $H_{c_{HB}}$, and mass flow rate, $\dot{M}$, are located at various distances from the arc heater and the readings recorded on magnetic tape are not actual arc heater conditions at the specific recording time. Separate mass flow vs. stagnation pressure curves for each arc heater, shown in Figure 9, are due to the different air injection systems used on the arc heaters. The six air injection jets of the N4000 arc heater, shown in Figure 2, have a total inlet area of .031 in^2 while the air injector ring of the N4001 arc heater (Figure 3) has a total inlet area of .013 in^2. The N4001 arc heater was designed to operate at lower air mass flow rates than the N4000 arc heater in order to obtain much higher bulk enthalpies at approximately equal power levels. Maximum deviations in nozzle exit static

pressures, as shown in Figure 10, indicate that the test core was not fully developed on several runs. P_{N_S} values in Table II show that there is no run-to-run predictability of the deviations.

B. 7.19 Inch Nozzle - Figure 11 presents measured mass flux and impact pressure profiles measured in the test section with the 7.19 inch nozzle system. Data for stagnation pressures of 150, 200, and 350 psia are shown, and calculated freestream velocity and density profiles were obtained from mass flux - impact pressure profiles. A test core radius of about 2 inches is seen from the measured data. A test core radius of approximately 2.9 inches was predicted using the method of Reference 6. A possible cause of the difference between predicted and measured test core size is the measuring probe influence on the test core as the probe is injected through the boundary layer. Predicted freestream velocities are somewhat higher than values calculated from tunnel measurements and calculated freestream densities are generally within the predicted range. It must be noted that predictions obtained from Ref. 6 are only rough estimates and are calculated for equilibrium or frozen nozzle flow. Also, steady one-dimensional flow with negligible heat transfer and viscous effects are assumed. Actual test cases presented in this report are nonequilibrium cases, and any or all assumptions made for the predictions may be violated. Accuracy of the mass flux measurements, while not determined precisely, is thought to be no greater than $\pm$10% as indicated by run-to-run variations in the test section profiles. No heat flux profiles were obtained while the 7.19 inch nozzle was in use, so local stagnation enthalpy calculations were not available.

Test section parameters presented in Figure 11 were obtained early in this program. Figure 12 presents later results. From these profiles it is apparent that the test core has not opened to the radius estimated by Ref. 6. Figure 12 shows minimum and maximum impact pressures for each stagnation pressure level to indicate the repeatability of the measurement. Maximum deviation in the test core was -5.2% to +3.2% at 350 psia stagnation pressure. The deviations are due partly to run-to-run variations in control parameters and partly to the accuracy of the instrumentation.

C. 19.36 Inch Nozzle - Because of its size and the ability to test larger models, the 19.36 inch exit diameter conical nozzle is the most extensively used configuration of the facility. Figure 13 presents averaged flow parameters which were obtained with the 19.36 inch nozzle at 4 stagnation pressure levels. A 200 psia stagnation pressure/6400 BTU/lb bulk stagnation enthalpy operating condition is shown with the three "standard" operating conditions.

Test section profiles presented in Figure 13 indicate a greater nozzle exit boundary layer than predicted by the method of Ref. 6. Several factors, such as nozzle wall temperature and surface roughness, would tend to create a different nozzle boundary layer in the real case than theory would predict. For instance, predictions were based on a laminar boundary layer in the nozzle while in the actual case copper oxides from the arc heater electrodes are deposited on the nozzle wall to create possible tripping of the boundary layer. Local stagnation enthalpies, freestream velocities and densities were calculated using measured values of mass flux, impact pressure and heat flux. These measurements were obtained from the edge of the nozzle exit, and the

assumption was made that symmetrical flow was produced in the conical nozzle.

Mass flow rates and bulk enthalpies were obtained by integrating mass flux and local enthalpy profiles for comparison with measured reservoir parameters. Integrated values,,presented in Figure 14, are seen to agree within $\pm$15 percent for both parameters. A major cause for disagreement between integrated and bulk values is the use of only eight widely spaced data points to obtain the flow profiles. Accuracy of the instrumentation used for the measurements, shown in Table I also contributes to the discrepancies.

Repeatability of the diagnostic probes is demonstrated in the data presented in Figure 15. Results presented for the 350 psia stagnation pressure condition are typical for the other conditions tested. Shaded symbols are average values from a total of 20 test runs made over a 3-year period. Lines showing maximum and minimum values of parameters are included. Poorest repeatability is shown in the mass flux profiles of Fig. 15a, where a $\pm$32 percent variation at the test section centerline is evident. A variation of -15.5% to +23.5% in centerline heat flux is seen in Figure 15c. The most repeatable parameter measured in the test section was impact pressure (Fig. 15b) where centerline values varied from the average by -5.5% to +7.6%. While some variation in the profiles is caused by run-to-run variations in operating conditions, condition of the probe tips and actual probe measurement fluctuations are major causes for measurement errors. After several runs the sharp leading edge of the mass flux probe tended to roll slightly because of heat and foreign objects in the airflow. This plus a buildup of deposits from the arc heater causes a change in the probe capture area and possible incomplete swallowing of the bow shock. While these effects are not

evident in impact pressure measurements, a slight change in the condition of the probe inlet geometry does contribute significantly to errors in mass flux measurements. A buildup of foreign material from the arc heater on the constantan foil surface of the heat flux gage also affected the measuring properties of that probe by changing the heat conduction properties of the gage. The impingement of solid particles of copper oxides on the face of the gage also causes high heat flux measurements. These particles are produced by the erosion of the copper electrodes in the arc heater and contribute unavoidable errors in aerodynamic heat flux measurements.

Because of the variations in diagnostic probe measurements, calibration data must be obtained during any test program being conducted in the 2 Ft EGF. Several calibration runs are made at the start of any test program and check points are obtained during the course of testing.

VI. CONCLUSIONS

From results presented in this report it is evident that several problems in maintaining stable operating conditions and measuring both test section and operating parameters remain to be solved and improved.

While stagnation pressure and arc heater current, the two set operating parameters, can be controlled, the resulting arc heater voltage and air mass flow rates are not controlled. The measurements of these parameters do not vary in a predictable manner. The amount of operating time on the electrodes, arc contact zones and methods and placement of parameter measuring equipment all affect voltage and mass flow measurements. Consequently, bulk stagnation enthalpy measurements, which depend on voltage and mass flow rates, could not be predicted with any consistency.

The method outlined in Reference 6 does not provide an accurate prediction of the test core. The assumptions are not sufficiently valid to use the technique for definition of test section parameters. The method is acceptable for defining parameters for pre-test planning.

Test section measurements vary to a larger degree than desired. The exact reason is not known. Contributing factors can be variance in operating conditions, heater and instrumentation error.

Of special concern is the measurement of mass flux, which exhibited the most random variation of the three test section parameters measured. Heat flux measurements also indicate that further improvements are needed to provide more consistent measurements.

Although random variations in measured test section parameters exist, meaningful test programs can still be conducted in the 2 Ft EGF by performing calibration check measurements in conjunction with the test program.

REFERENCES

1. Beachler, John C., "Design and Shakedown Operation of the Air Force Flight Dynamics Laboratory's 2 Ft (4 Megawatt) Electro-Gasdynamic Facility", FDM-TM-68-3, July 1968.

2. Zonars, Demetrius, "Theoretical and Experimental Study of Equilibrium and Non-Equilibrium Air Flow through a M=10 Contoured Nozzle", Ph.D Thesis, The Ohio State University, June 1965.

3. Hillsamer, M.E., "Results of Calibration Tests Conducted in the AFFDL Two Foot Electrogasdynamics Facility", Paper prepared for the thirty-first semiannual meeting of the Supersonic Tunnel Association (closed session), 24-25 Apr. 1969.

4. Little, Floyd W. "2 Ft Electrogasdynamic Facility Status", AFFDL/FXN, 1 October 1970.

5. Parobek, Daniel M., "Performance of Free Stream Flow Instrumentation for 9-Inch Contoured Nozzle Test in the RTD 4-Megawatt Electro Gasdynamic Facility", AFFDL-TR-65-179, December 1965.

6. Mann, Capt Micheal J. and Rockwell, William A., "A Rapid Method of Computing Hypersonic Wind Tunnel Test Section Flow Conditions with Application to the AFFDL Two-Foot Electro-Gasdynamic Facility", AFFDL-TR-66-185, August 1967.

7. Burke, A.F., Smith, W.E., Dowling, E.D. and Carlson, D.R. "Lifting Surfaces in Rarified Hypersonic Airflow, Part I: The Effects of Bluntness and Angle of Attack on the Flow Over a Flat Plate", ASD-TDR-62-797, Part I, Cornell Aeronautical Laboratory, Inc., Buffalo, New York, February 1963.

Table I Facility and Test Section Instrumentation

Item	Symbol	Identity	Remarks	Accuracy
1	P_o	Stagnation Pressure, psia	Measured by 1000 psia transducer at arc heater anode	±5% of reading
2	I	Arc current, amps	Measured by shunt calibrated to 2500 amps in grounded main bus and transductor system	
3	E	Arc voltage, volts	0–10000 volts measured by calibrated voltage divider connected from hot to grounded bus	
4	$\dot{M}$	Air mass flow rate, lb/sec	Computed from air supply line pressure and temperature, differential pressure across metering orifice and a precalibrated orifice coefficient	
5	P_{LU}	Supply line pressure, psia	Measured by 3000 psia transducer located upstream of mass flow metering orifice	±5% of reading
6	T_{LU}	Supply Line temperature, deg R	Iron/constantan thermocouple located upstream of mass flow orifice	±1 deg R
7	ΔP	Mass flow differential pressure, psid	Measured by 4 psid transducer across mass flow orifice	

Table I (Continued)

Item	Symbol	Identity	Remarks	Accuracy
8	F_{M1}	Rear electrode coolant flow rate, gpm	Measured by turbine type flowmeter, 0-300 gpm	±5% of reading
9	F_{M2}	Swirl chamber coolant flow rate, gpm	Measured by turbine type flowmeter, 0-125 gpm	±5% of reading
10	F_{M3}	Front electrode coolant flow rate, gpm	Measured by turbine type flowmeter, 0-600 gpm	±5% of reading
11	F_{M4}	Nozzle throat coolant flow rate, gpm	Measured by turbine type flowmeter, 0-125 gpm	±5% of reading
12	ΔT_1	Rear electrode coolant temp. rise, °R	Measured by "Delta T" sensor, 0-90°R	±1 deg R
13	ΔT_2	Swirl chamber coolant temp. rise, °R	Same as item 12	Same as item 12
14	ΔT_3	Front electrode coolant temp. rise, °R	Same as item 12	Same as item 12
15	ΔT_4	Nozzle throat coolant temp. rise, °R	Same as item 12	Same as item 12
16	T_1	Arc heater coolant supply temp., °R	Measured by iron/constantan thermocouple in coolant supply line.	±1 deg R
17	F_{M5}	Effuser coolant flow rates, gpm	Measured by a turbine type flow meter in effuser coolant flow line, 0-125 gpm	±5% of reading
18	ΔT_5	Effuser coolant temp. rise deg R	Measured by a "Delta T" sensor in effuser coolant flow line, 0-90°R	±1 deg R

Table I (Continued)

Item	Symbol	Identity	Remarks	Accuracy
19	P_{Ns}	Nozzle exit static pressure, Torr	Pressure tap at nozzle exit connected to 0-5 Torr thermocouple gage	±5% of reading
20	P_{Tc}	Test cabin static pressure, Torr	Pressure tap in test cabin sidewall connected to 0-5 Torr thermocouple gage	±5% of reading
21	ET	Elapsed Time	0-10 minute analog dock starts at initial tunnel start	
22	V_M	Model radial position	Analog signal from potentiometer	±0.2 in.
23	V_{pr1}	Probe 1 radial position	Analog signal from potentiometer	±0.1 in.
24	V_{pr2}	Probe 2 radial position	Analog signal from potentiometer	±0.1 in.
25	$(\rho u)_\infty$	Test section local mass flux, lb/sec	Mass flux probe and D.W. Young flowmeter 1.5×10^{-3} to 1.0 lb/ft^2 sec	±10% of reading
26	P_{T2}	Local impact pressure, Torr	Mass flux probe and 300 Torr absolute pressure transducer	±2% of reading
27	$\dot{q}_{ssc}$	Local heat flux	Gardon type heat flux gage mounted in 1 in. dia. hemisphere cylinder probe	±10% of reading

Table II. Tunnel Run Average Conditions

Run Nr.	P_o psia	$H_{o\,NB}$ BTU/lbm	I_{Arc} amps	E_{Arc} volts	$\dot{m}$ lb/sec	P_{NS} mm Hg	Heater	D_{NE} inches
68-55	154	3632	262	2243	.116	1.100	N4000	7.19
68-60	149	2586	237	2225	.111	—	N4000	7.19
68-61	147	2484	240	2149	.108	—	N4000	7.19
68-62	149	2774	253	2176	.108	—	N4000	7.19
68-63	148	2561	261	2114	.106	—	N4000	7.19
68-64	149	2872	265	2090	.104	.978	N4000	7.19
68-65	152	3025	285	2108	.110	.949	N4000	7.19
68-70	151	2902	274	2072	.106	1.006	N4000	7.19
68-87	156	6520	1206	900	.080	.843	N4001	7.19
68-88	149	4986	1185	753	.085	.805	N4001	7.19
68-89	146	4838	1195	723	.087	.849	N4001	7.19
68-92	150	5178	1204	750	.083	.849	N4001	7.19
68-94	152	4568	1230	780	.088	.912	N4001	7.19
68-95	152	4743	1238	752	.088	.893	N4001	7.19
68-97	146	4996	1218	730	.086	.902	N4001	7.19
68-57	204	2618	284	2709	.160	1.495	N4000	7.19
68-57	200	2701	293	2547	.150	1.423	N4000	7.19
68-66	196	2975	290	2574	.142	1.332	N4000	7.19
68-18	200	4915	1213	874	.110	1.076	N4001	7.19
68-27	202	6208	1238	1136	.114	1.313	N4001	7.19
72-68	249	5616	1786	1006	.143	1.475	N4001	7.19
72-69	249	—	1777	—	—	—	N4001	7.19
72-72	249	6310	1790	999	.131	1.860	N4001	7.19
72-73	248	6408	1784	989	.130	1.825	N4001	7.19
72-74	248	6000	1794	924	.126	1.646	N4001	7.19
72-75	248	5667	1778	889	.126	1.717	N4001	7.19
68-84	349	3218	548	3248	.268	2.878	N4000	7.19
68-85	346	3093	532	3288	.268	2.878	N4000	7.19
68-86	344	3400	552	3420	.288	3.068	N4000	7.19
68-81	348	3192	579	2958	.240	2.309	N4000	7.19
68-82	350	3565	590	3020	.250	2.356	N4000	7.19
68-83	346	3654	594	3040	.254	2.338	N4000	7.19
68-99	348	2524	578	2792	.264	2.348	N4000	7.19
68-100	350	2515	578	2803	.266	2.349	N4000	7.19
68-101	352	2594	591	2810	.270	2.353	N4000	7.19

Table II. (Continued)

Run Nr.	P_o psia	H_{oHB} BTU/lbm	I_{Arc} amps	E_{Arc} volts	$\dot{m}$ lb/sec	P_{NS} mm Hg	Heater	D_{NE} inches
72-55	351	3493	745	2763	.268	2.288	N4000	7.19
72-56	349	3416	747	2739	.269	2.300	N4000	7.19
72-57	351	3580	746	2787	.260	2.382	N4000	7.19
72-58	353	3492	743	2746	.262	2.548	N4000	7.19
72-59	350	3473	730	2788	.266	2.486	N4000	7.19
72-60	352	3458	750	2775	.255	2.119	N4000	7.19
72-61	349	3153	752	2589	.267	2.298	N4000	7.19
72-62	349	3088	747	2653	.271	2.317	N4000	7.19
72-63	498	2129	516	3764	.451	3.362	N4000	7.19
72-64	501	2132	552	3601	.446	3.551	N4000	7.19
72-65	497	3972	536	4914	.355	3.708	N4000	7.19
72-66	497	3923	534	4877	.357	3.614	N4000	7.19
72-67	495	3768	533	4777	.357	3.628	N4000	7.19
68-127	199	8071	1823	994	.099	.174	N4001	19.36
68-128	199	7156	1786	926	.098	.207	N4001	19.36
68-129	198	6706	1760	808	.104	.192	N4001	19.36
68-130	199	6595	1814	771	.102	.249	N4001	19.36
68-131	200	6546	1821	738	.096	.175	N4001	19.36
68-132	198	6834	1822	746	.094	.277	N4001	19.36
68-133	200	6720	1824	736	.093	.145	N4001	19.36
68-134	197	7122	1852	737	.092	.154	N4001	19.36
68-135	203	8141	1820	925	.096	.145	N4001	19.36
68-136	199	7987	1820	920	.098	.152	N4001	19.36
68-137	200	—	1824	797	.096	.134	N4001	19.36
68-138	201	6678	1810	770	.106	.167	N4001	19.36
69-137	203	6686	1819	821	.108	.131	N4001	19.36
69-138	203	6776	1802	814	.102	.151	N4001	19.36
69-139	200	6821	1806	791	.099	.177	N4001	19.36
69-140	199	6283	1795	783	.101	.090	N4001	19.36
69-141	203	6343	1816	786	.107	.162	N4001	19.36
69-142	201	6337	1809	787	.108	.151	N4001	19.36
69-143	204	6271	1793	808	.107	.210	N4001	19.36
69-146	202	8156	1797	1004	.103	.155	N4001	19.36
69-147	196	7202	1796	817	.097	.176	N4001	19.36
69-148	196	7186	1794	817	.096	.131	N4001	19.36
69-154	198	4868	1793	814	.098	.133	N4001	19.36
69-155	198	4613	1805	786	.094	.129	N4001	19.36
69-158	200	7783	1810	962	.104	.131	N4001	19.36
71-52	192	5397	1787	855	.114	.308	N4001	19.36
71-53	194	6385	1797	862	.098	.155	N4001	19.36

Table II. (Concluded)

Run Nr.	P_o psia	H_{oHB} BTU/lbm	I_{Arc} amps	E_{Arc} volts	$\dot{m}$ lb/sec	P_{NS} mm Hg	Heater	D_{NE} inches
70-44	248	5735	1792	973	.125	.188	N4001	19.36
70-47	249	5724	1793	860	.127	.174	N4001	19.36
70-48	253	5469	1786	848	.129	.186	N4001	19.36
70-49	247	5474	1792	825	.127	.147	N4001	19.36
71-55	243	6517	1799	1045	.131	.231	N4001	19.36
71-56	249	6778	1802	1134	.129	.185	N4001	19.36
71-57	245	7049	1792	1129	.126	.196	N4001	19.36
71-58	246	6399	1780	1064	.129	.165	N4001	19.36
71-59	249	6461	1787	1079	.131	.206	N4001	19.36
69-104	345	—	754	2530	.235	.232	N4000	19.36
69-105	350	2972	755	2721	.244	.209	N4000	19.36
69-110	352	2915	760	2731	.235	.265	N4000	19.36
69-111	351	2973	747	2761	.248	.222	N4000	19.36
69-118	350	2627	736	2658	.249	.284	N4000	19.36
69-120	350	2689	755	2666	.233	.240	N4000	19.36
69-125	348	3072	754	2705	.224	.250	N4000	19.36
69-126	345	3268	764	2699	.234	.306	N4000	19.36
70-3	350	3575	743	2790	.234	.169	N4000	19.36
70-4	349	4024	748	2822	.211	.259	N4000	19.36
70-5	350	3889	744	2787	.212	.268	N4000	19.36
70-6	346	3804	744	2732	.211	.353	N4000	19.36
70-7	346	3623	763	2729	.213	.243	N4000	19.36
70-8	347	3637	774	2721	.216	—	N4000	19.36
70-20	347	3178	744	2630	.221	.224	N4000	19.36
70-21	346	3152	737	2639	.224	.205	N4000	19.36
71-34	347	3790	760	2984	.254	—	N4000	19.36
71-38	353	3108	764	2858	.272	.262	N4000	19.36
71-49	349	3503	740	2782	.245	.259	N4000	19.36
71-50	347	3364	742	2745	.248	.267	N4000	19.36
69-112	506	2231	559	3936	.404	.307	N4000	19.36
69-114	499	2137	544	3463	.356	.234	N4000	19.36
69-119	496	2231	532	3897	.376	.332	N4000	19.36
69-121	501	2372	555	3888	.380	.322	N4000	19.36
71-41	497	2343	538	3977	.408	.356	N4000	19.36
71-42	495	3073	541	4028	.322	.312	N4000	19.36
71-43	495	2503	547	4041	.400	.348	N4000	19.36
71-46	495	2449	547	3979	.405	.339	N4000	19.36
71-47	492	2550	554	4000	.403	.348	N4000	19.36
71-48	494	2408	543	4041	.417	.351	N4000	19.36

TABLE III. COMPARISON OF DESIRED AND ACTUAL TEST CONDITIONS

DESIRED CONDITIONS				ACTUAL CONDITIONS			
D_{NE} inches	P_o psia	$H_{o_{HB}}$ BTU/lb$_m$	$\dot{m}$ lb/sec	P_o psia	$H_{o_{HB}}$ BTU/lb$_m$	$\dot{m}$ lb/sec	Remarks
7.19	250	7000	.125	248	4422	.126	Min.
				249	5737	.131	Average
				249	6408	.143	Max
	350	3500	.265	349	3088	.260	Min.
				350	3394	.265	Average
				353	3580	.271	Max.
	500	2500	.375	495	2129	.355	Min.
				498	3185	.393	Average
				501	3972	.451	Max.
19.36	250	7000	.125	242	5469	.125	Min.
				248	6178	.128	Average
				253	7049	.131	Max.
	350	3500	.265	345	2627	.211	Min
				350	3226	.235	Average
				353	4024	.272	Max.
	500	2500	.375	493	2137	.266	Min.
				497	2430	.378	Average
				506	3073	.417	Max

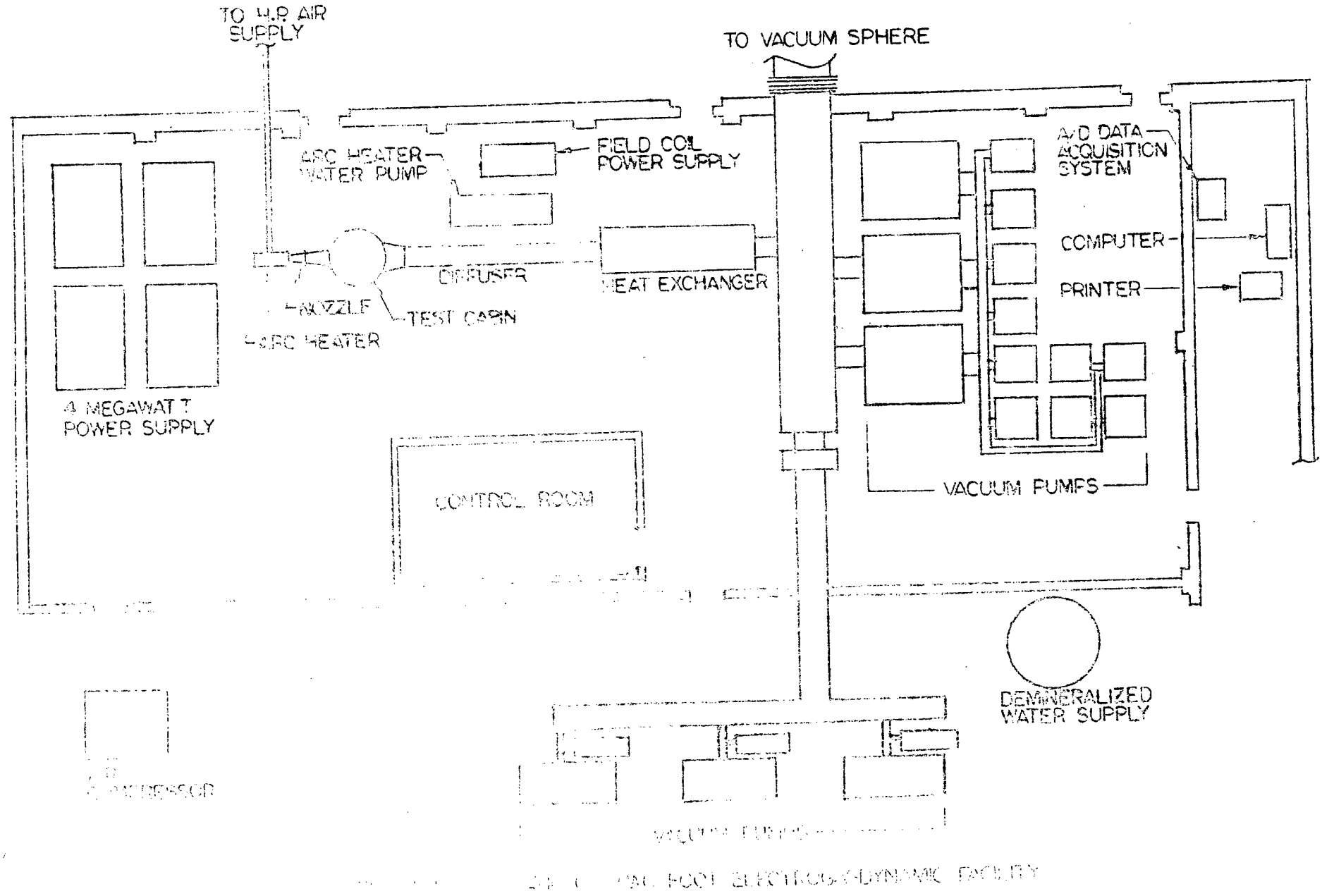
TO H.P AIR SUPPLY
TO VACUUM SPHERE
ARC HEATER WATER PUMP
FIELD COIL POWER SUPPLY
A/D DATA ACQUISITION SYSTEM
COMPUTER
PRINTER
DIFFUSER
HEAT EXCHANGER
NOZZLE
TEST CABIN
ARC HEATER
4 MEGAWATT POWER SUPPLY
CONTROL ROOM
VACUUM PUMPS
DEMINERALIZED WATER SUPPLY

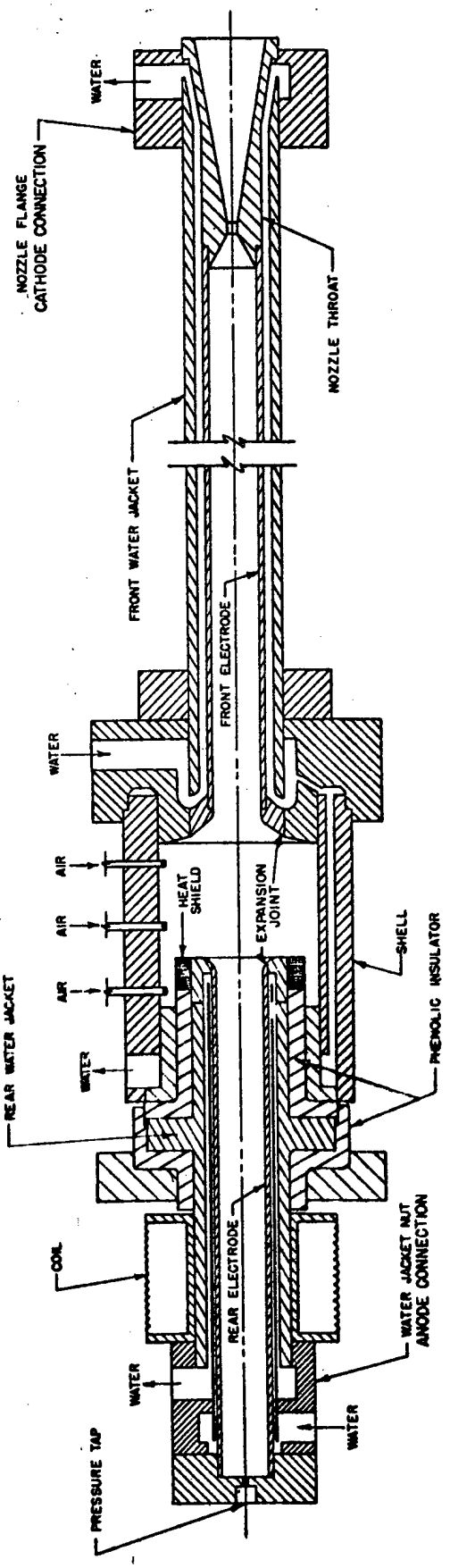

FIGURE 2. H-4000 ARC AIR HEATER CROSS SECTION VIEW

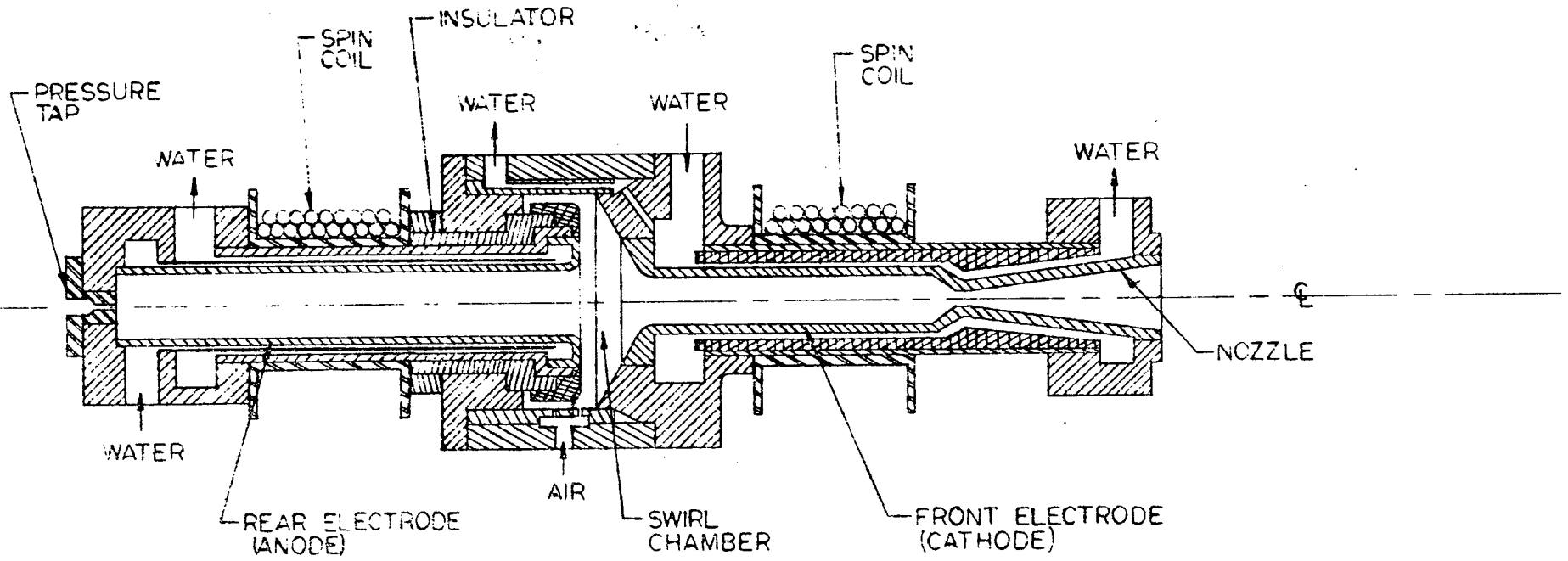

FIGURE 3 H-420W Arc Jet Heater Cross Section View

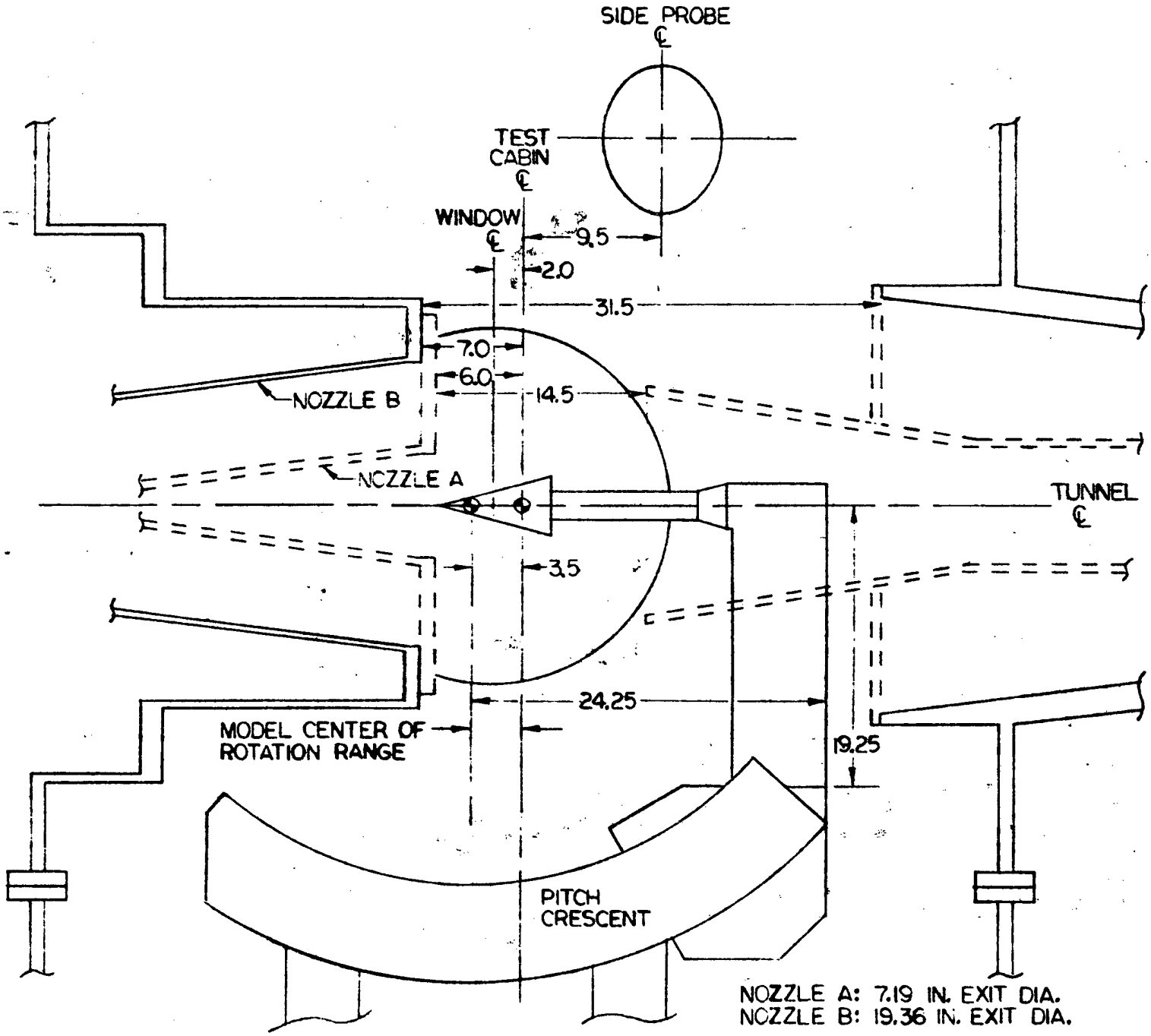

FIGURE 4. TEST CABIN SCHEMATIC

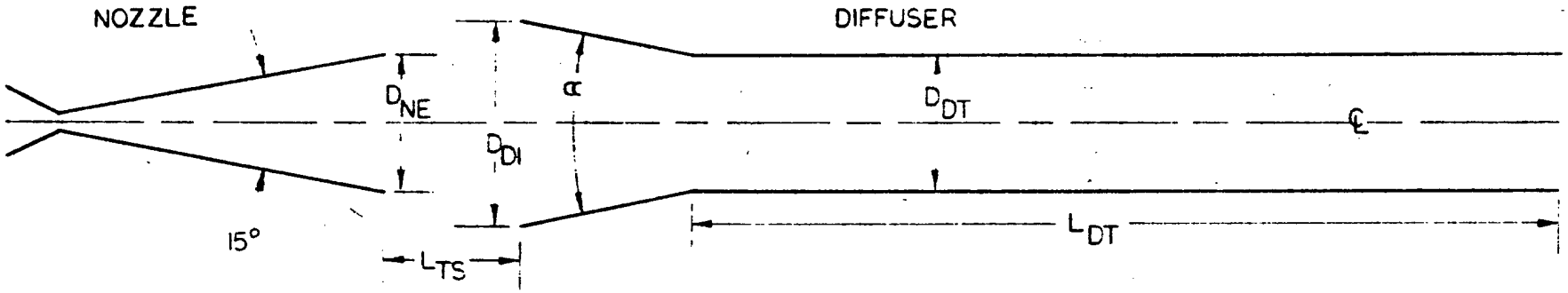

ALL DIMENSIONS ARE IN INCHES

TUNNEL CONFIGURATION	D_{NE}	D_{DT}	$\frac{AREA_{DT}}{AREA_{NE}}$	L_{DT}	$\frac{L_{DT}}{D_{DT}}$	$\frac{L_{TS}}{D_{NE}}$	D_{DI}	α
I	7.19	8.0	1.24	160.0	20.0	2.02	15.0	18°
II	19.36	21.0	1.18	255.0	12.1	1.65	24.0	8°
III	19.36	22.0	1.29	327.5	14.9	1.63	28.5	14°

FIGURE 5. TUNNEL CONFIGURATIONS

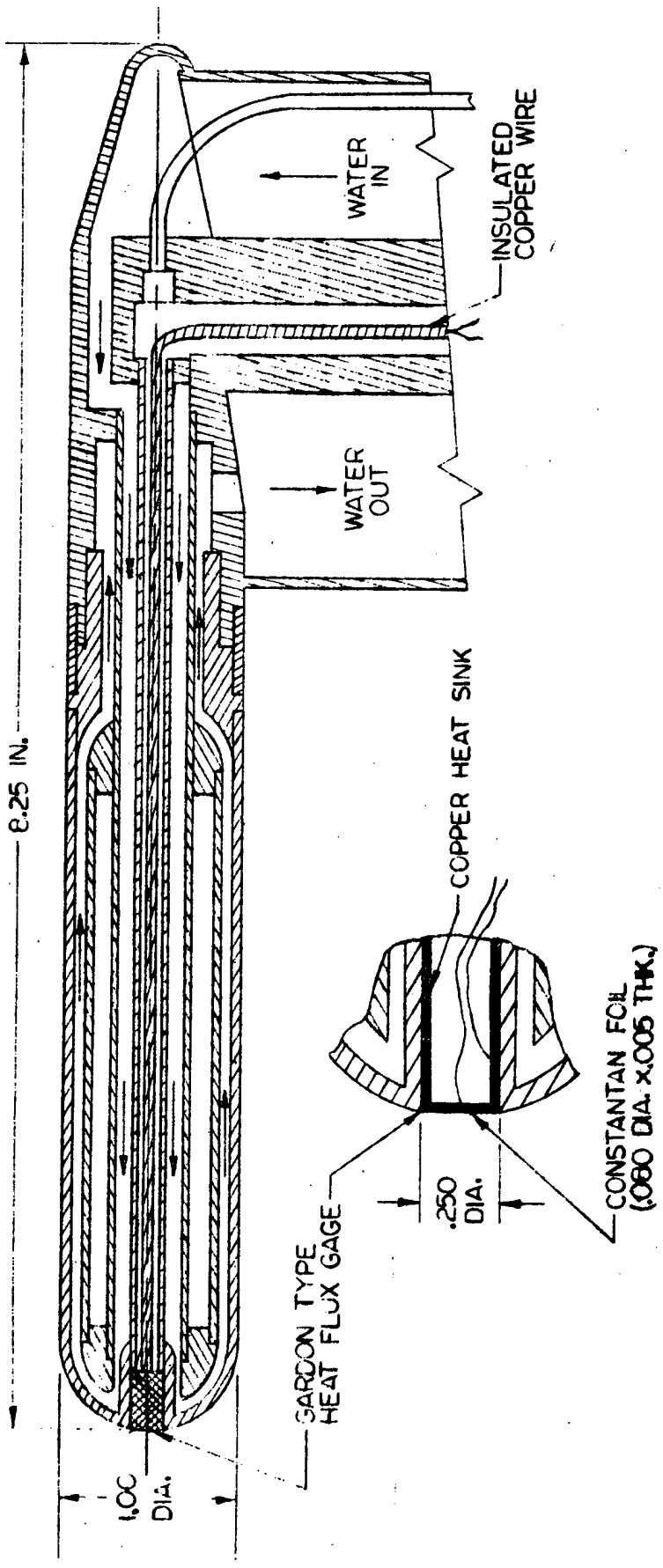

FIGURE 6. HIGH RESPONSE STEADY STATE CALORIMETER

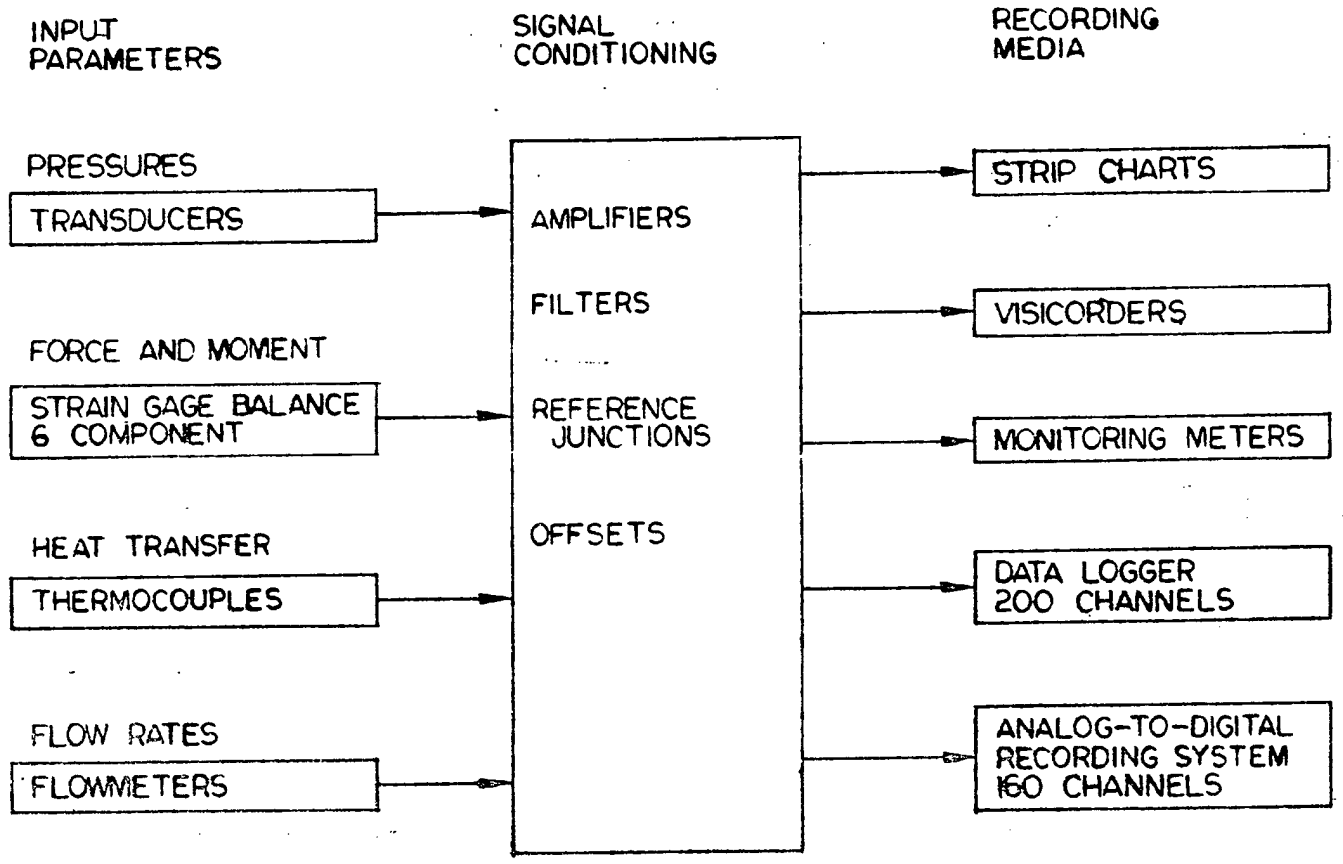

FIGURE 7. SCHEMATIC OF DATA PROCESSING SYSTEM

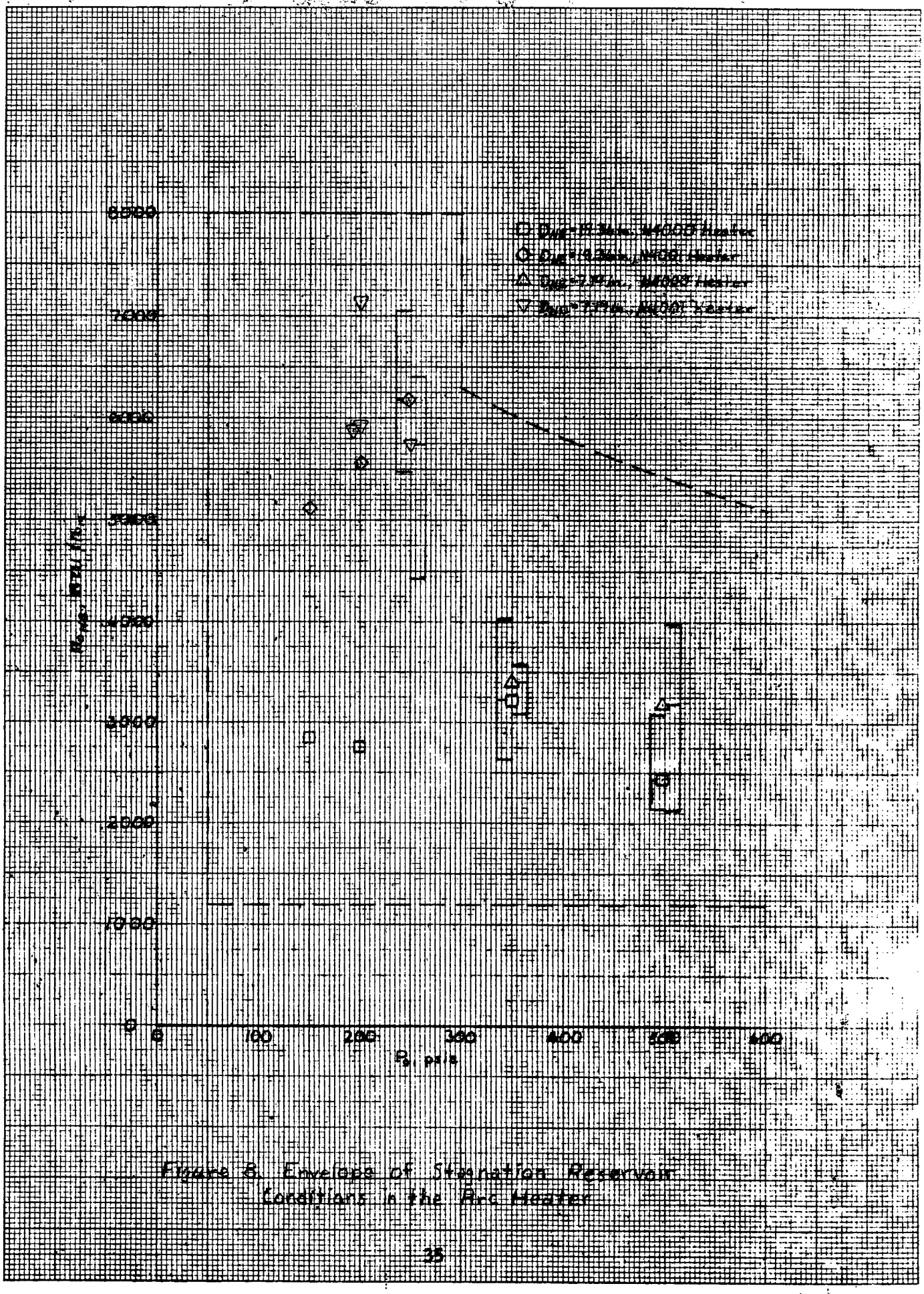

Figure 8. Envelope of Stagnation Reservoir Conditions in the Arc Heater

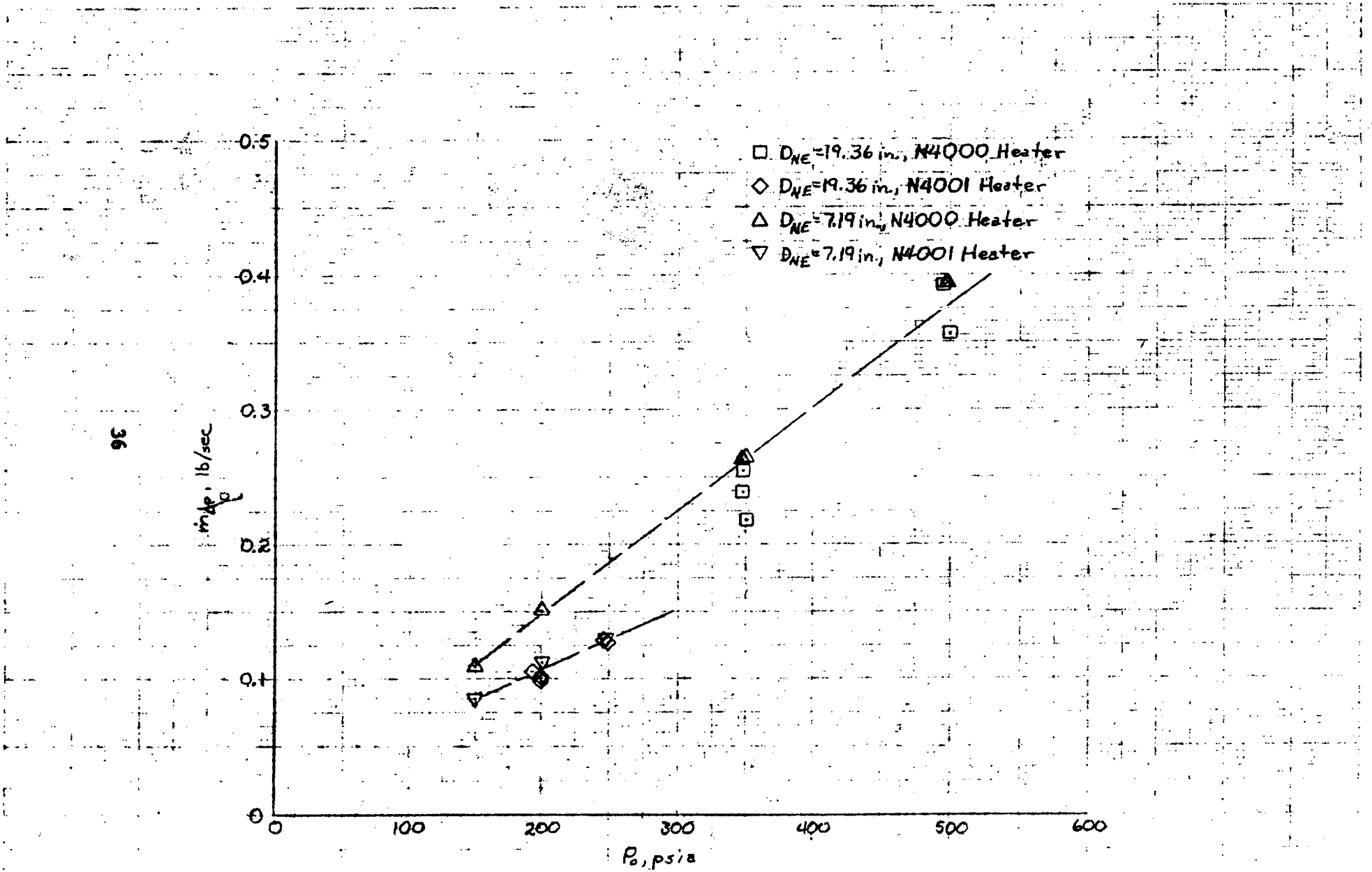

Figure 9. Average Mass Flow Rates versus Stagnation Pressures

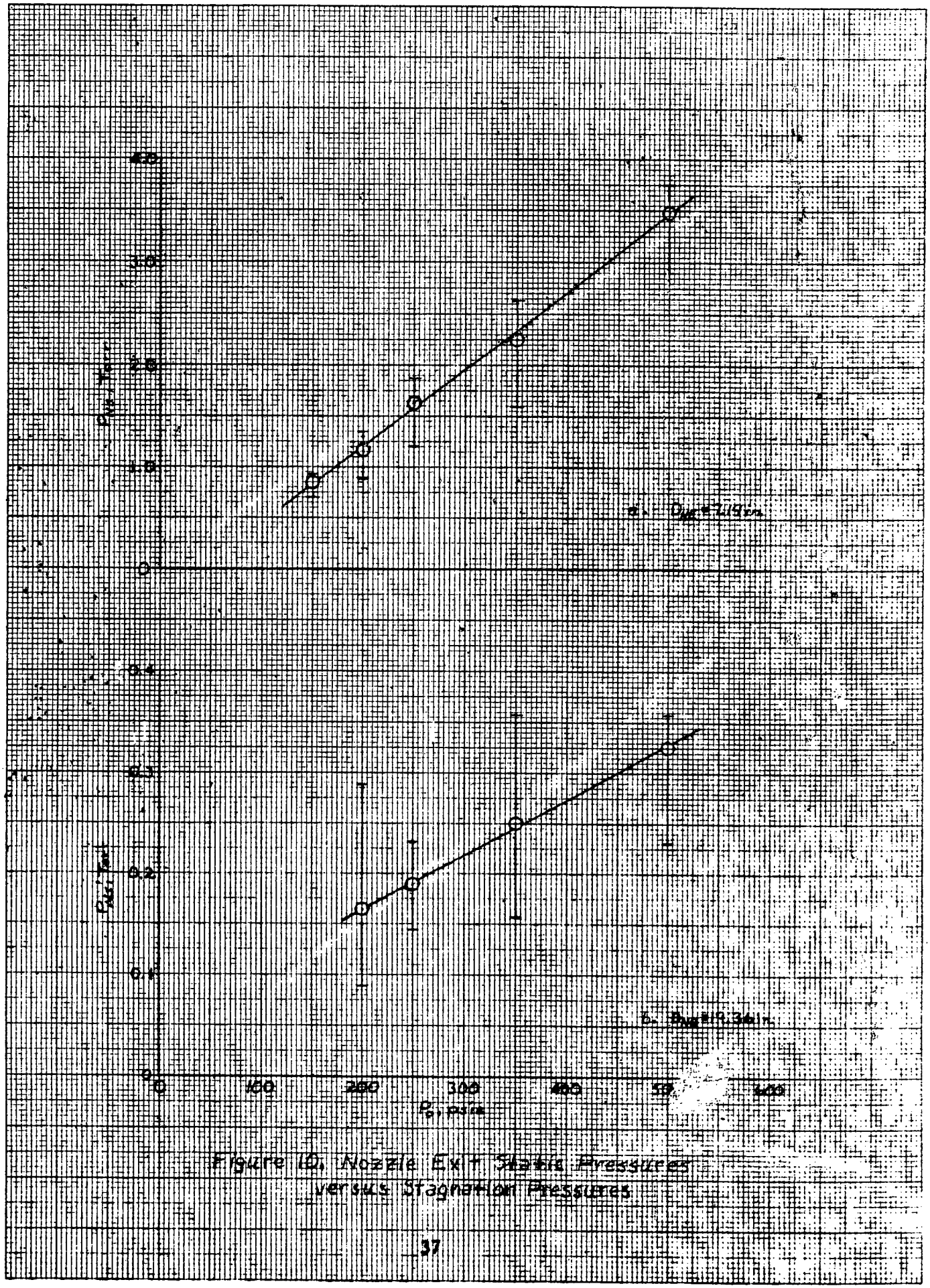

Figure 10. Nozzle Exit Static Pressures versus Stagnation Pressures

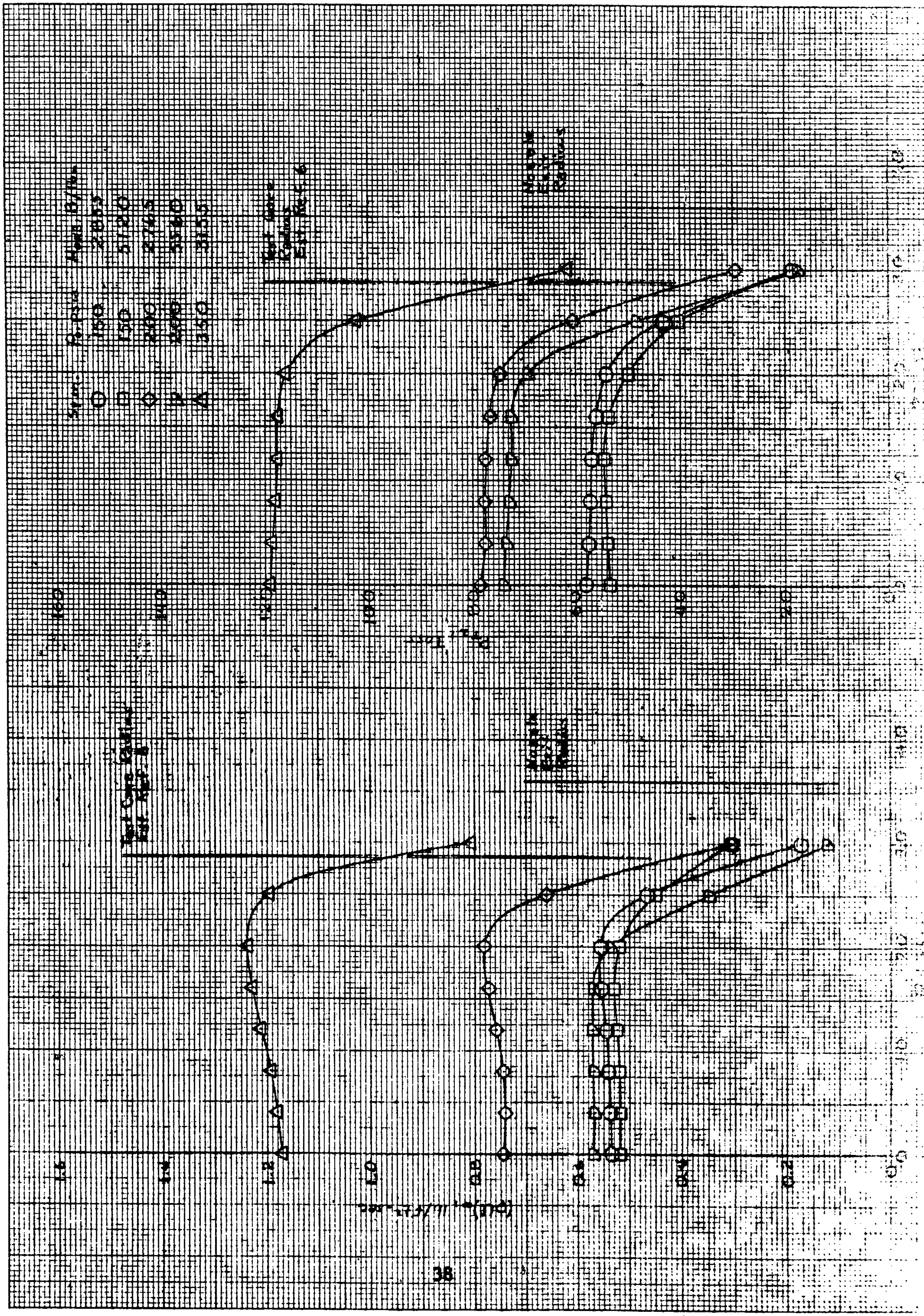

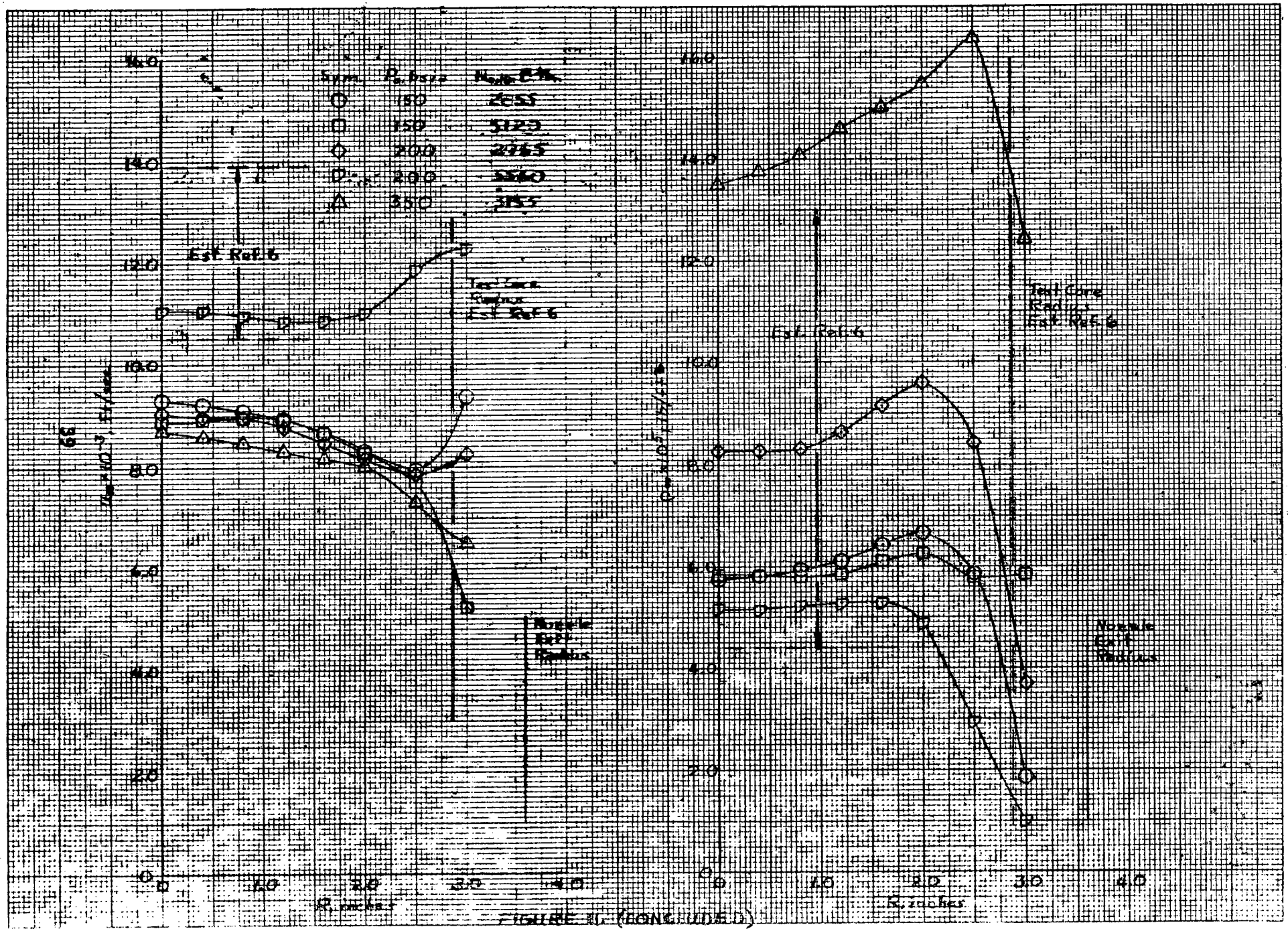

FIGURE 10. (CONCLUDED)

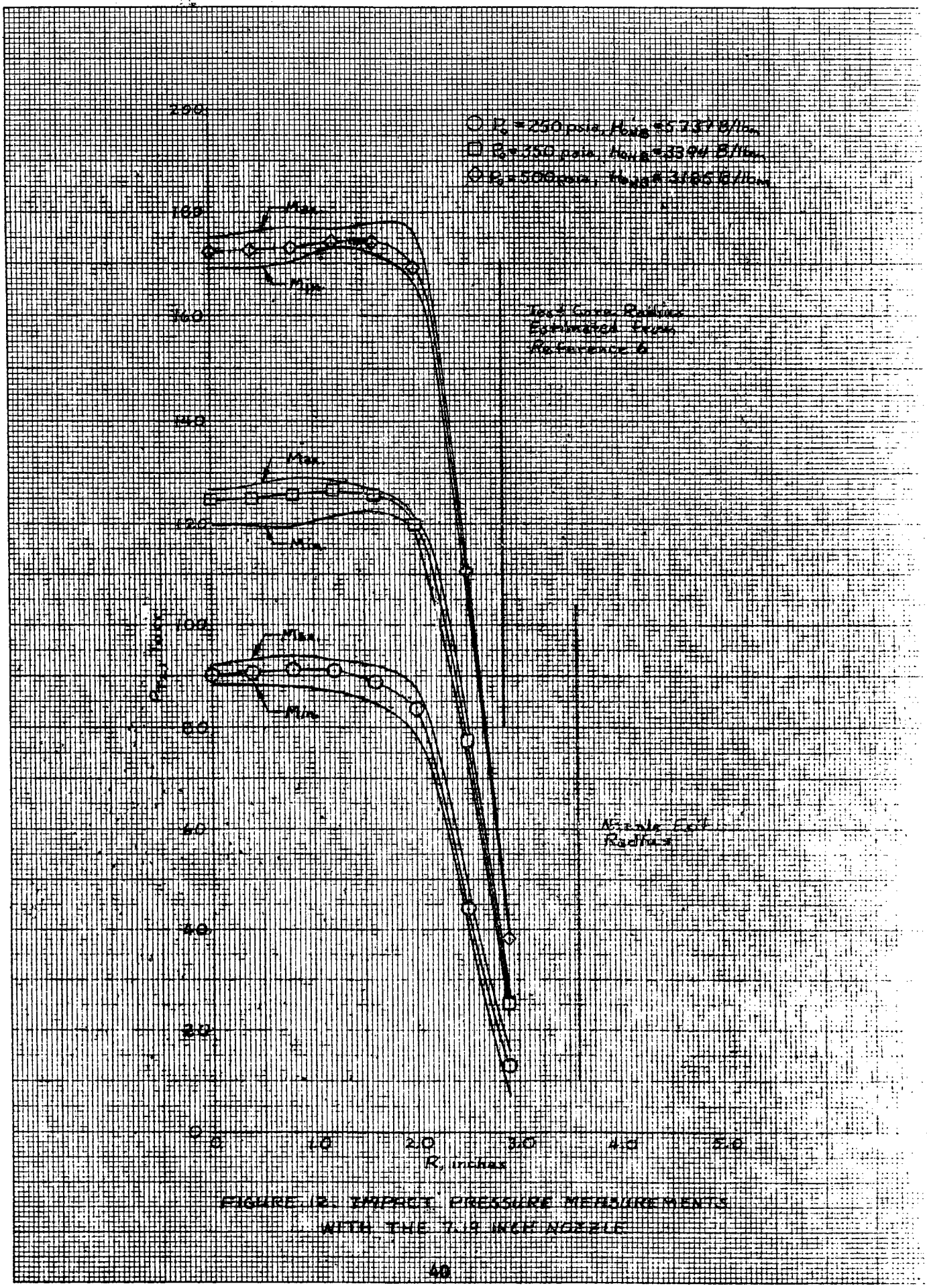

FIGURE 12. IMPACT PRESSURE MEASUREMENTS WITH THE 7.9 INCH NOZZLE

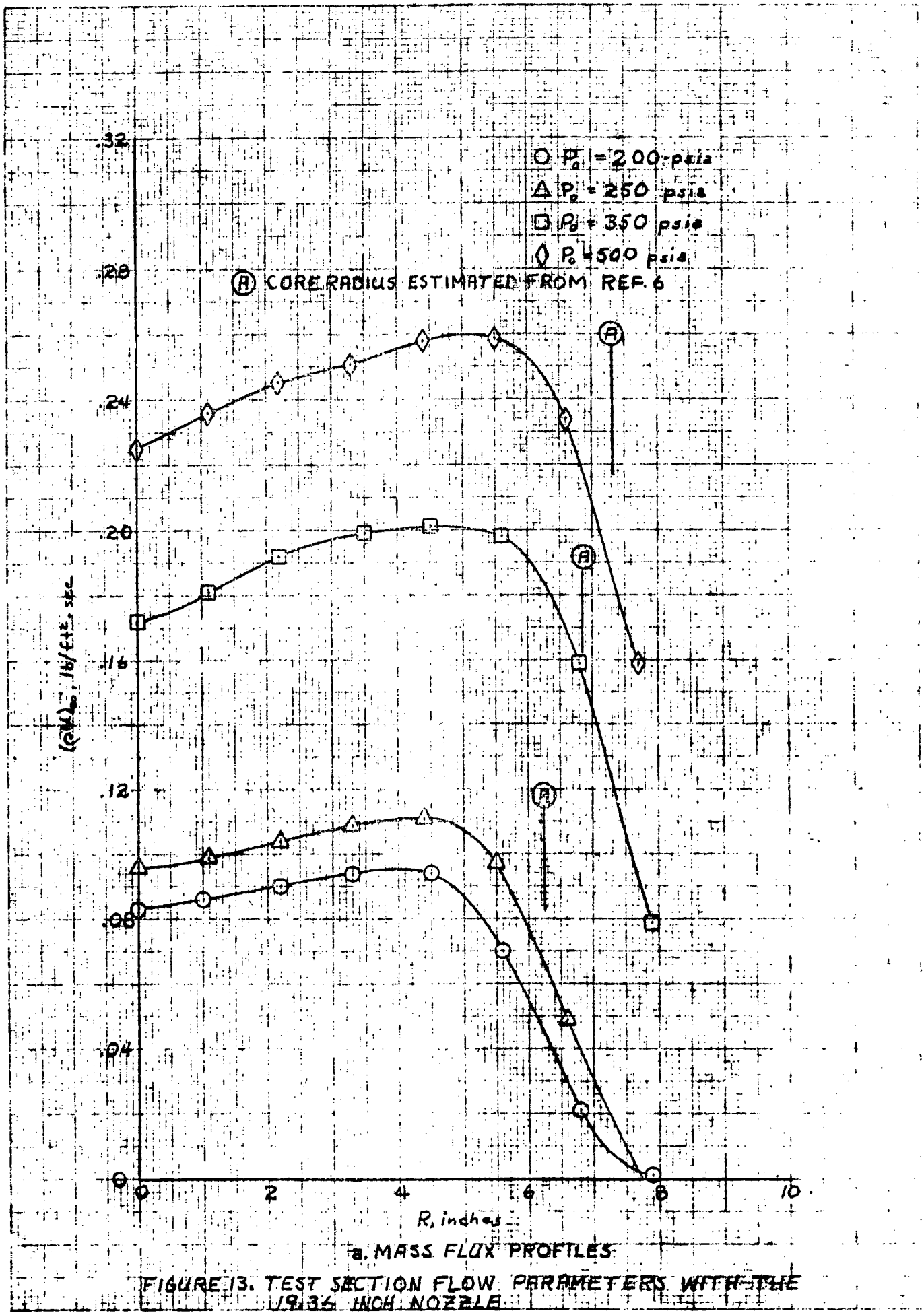

a. MASS FLUX PROFILES

FIGURE 13. TEST SECTION FLOW PARAMETERS WITH THE 1.9136 INCH NOZZLE

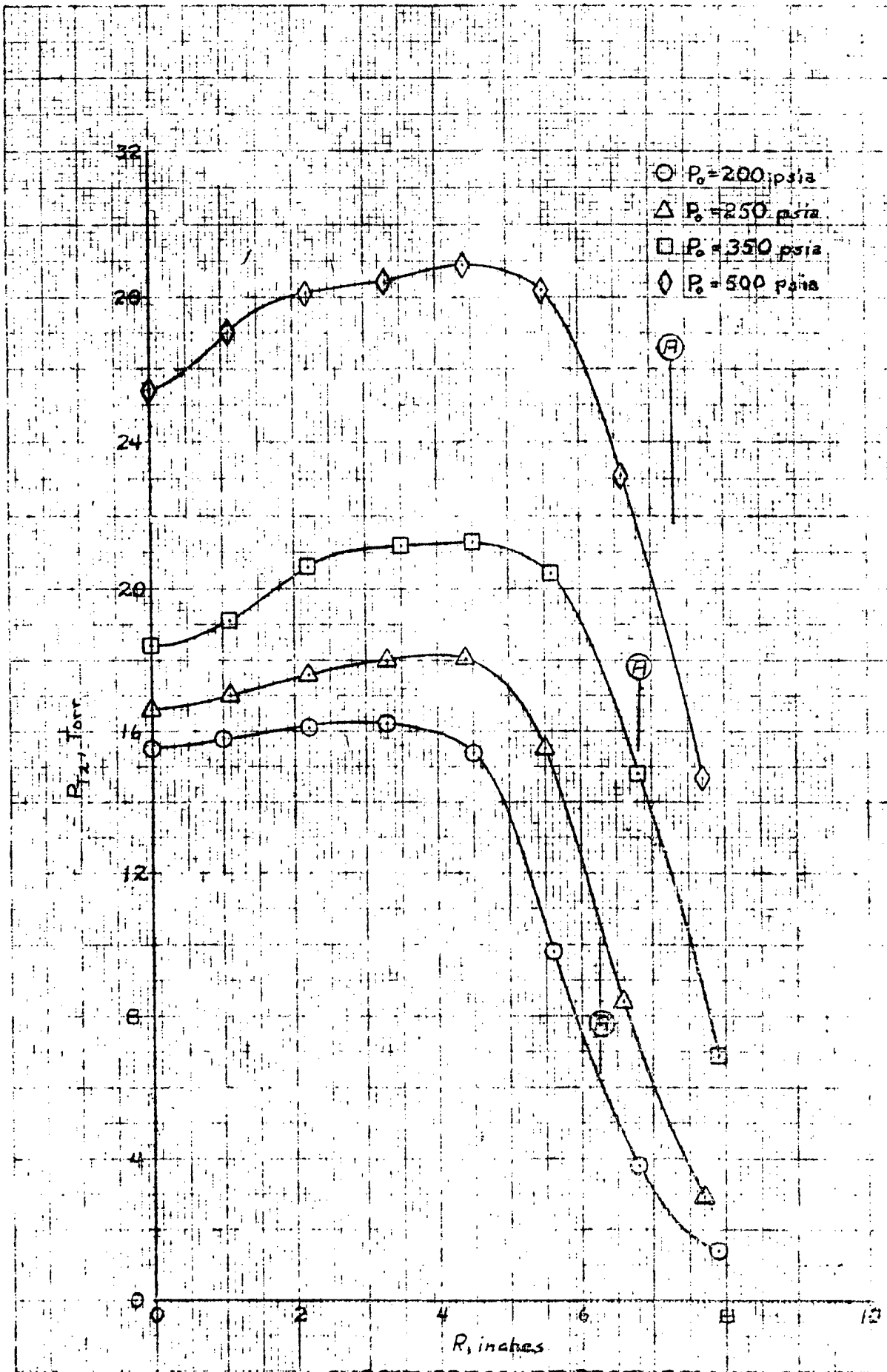

b. IMPACT PRESSURE PROFILES

FIGURE 13. (CONTINUED)

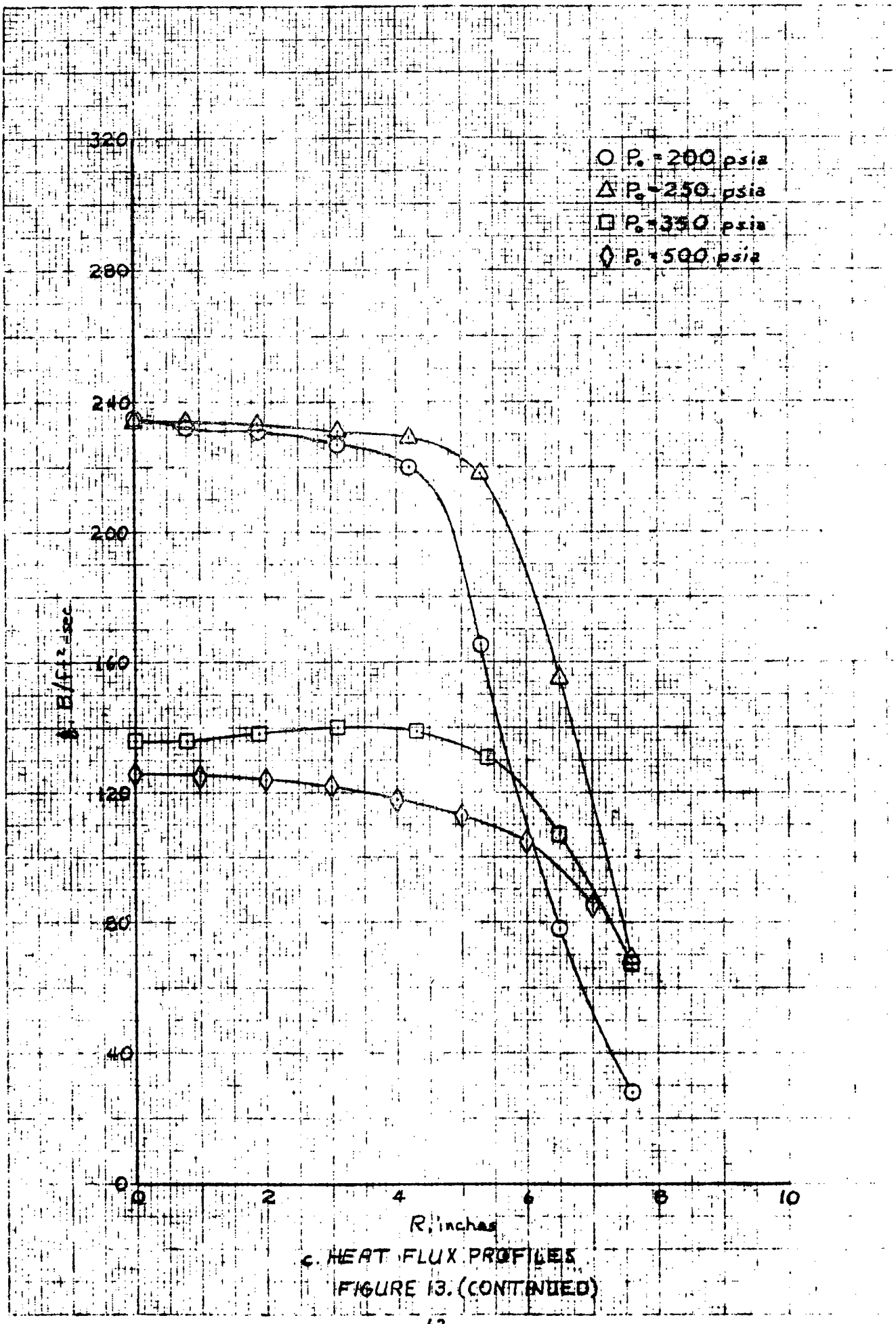

c. HEAT FLUX PROFILES

FIGURE 13. (CONTINUED)

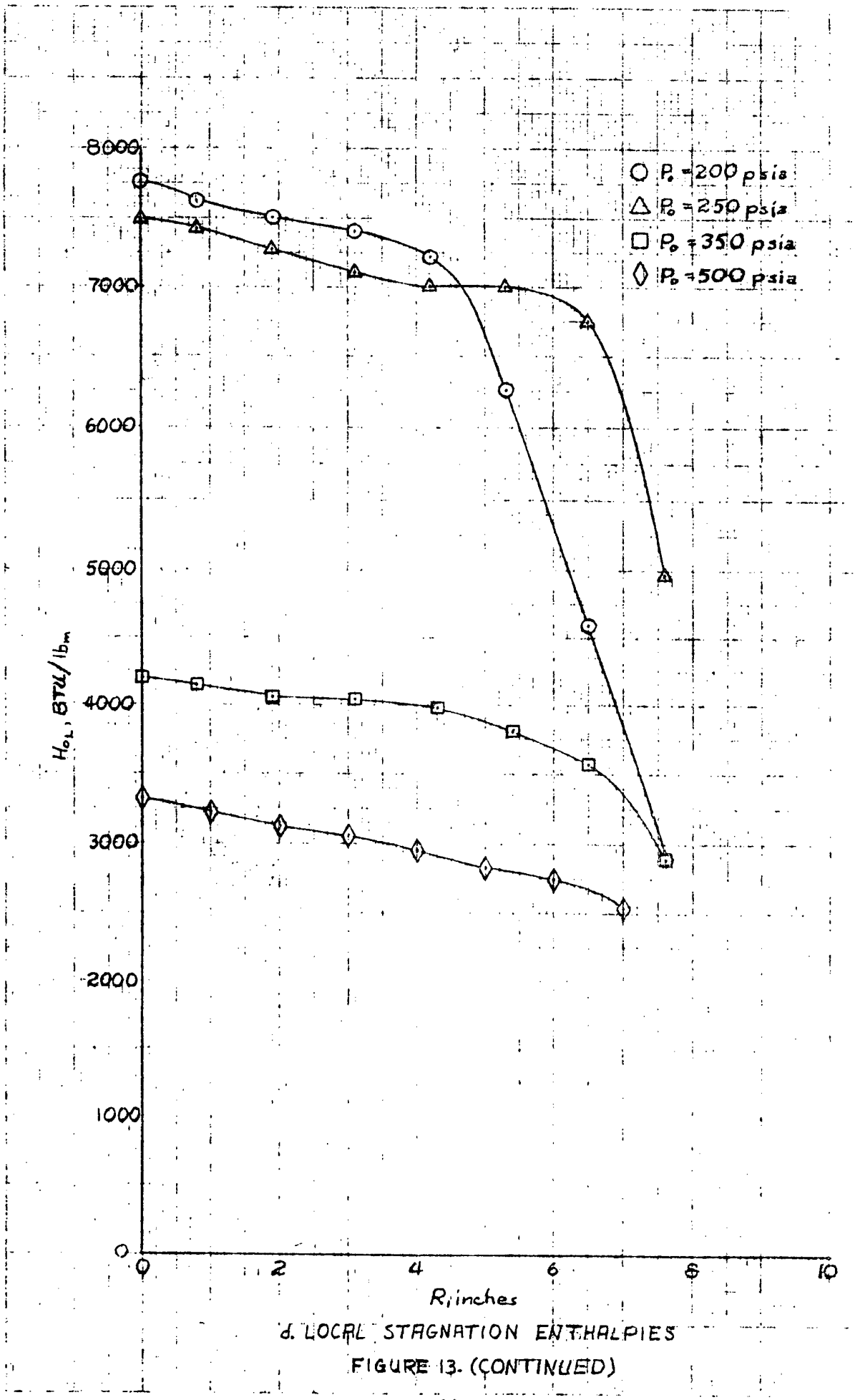

d. LOCAL STAGNATION ENTHALPIES

FIGURE 13. (CONTINUED)

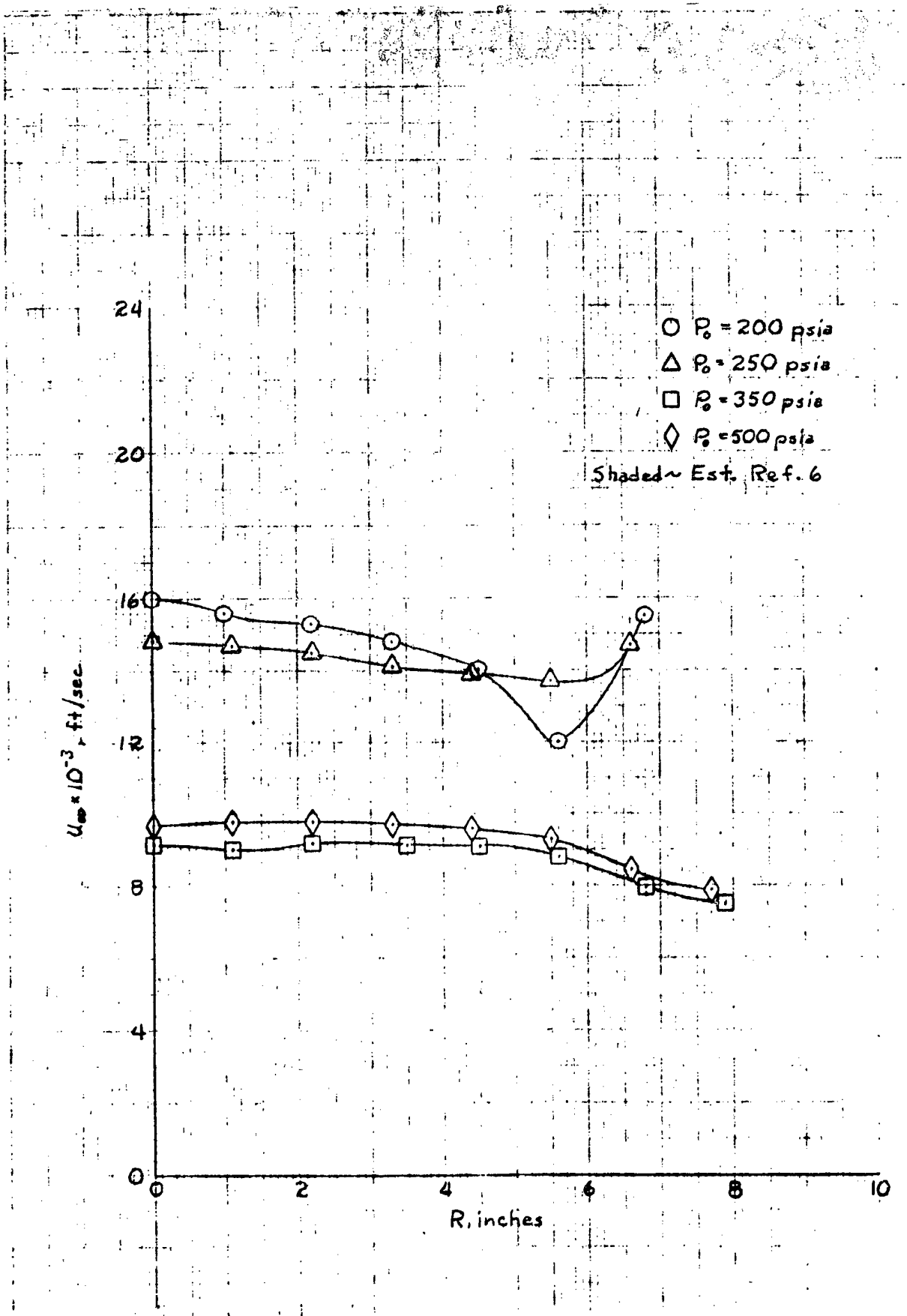

e. LOCAL FREESTREAM VELOCITIES

FIGURE 13. (CONTINUED)

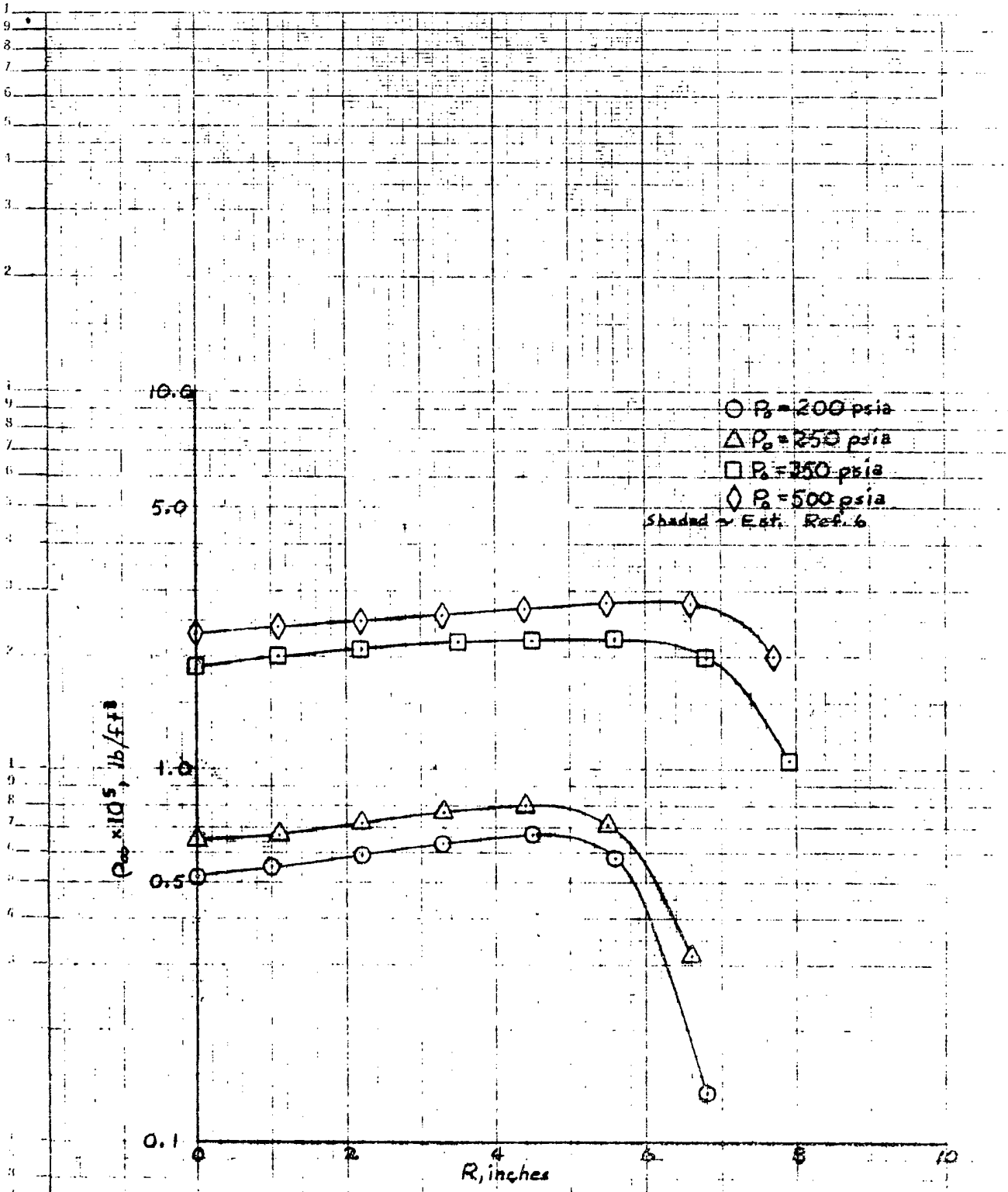

E. LOCAL FREESTREAM DENSITIES

FIGURE 13. (CONCLUDED)

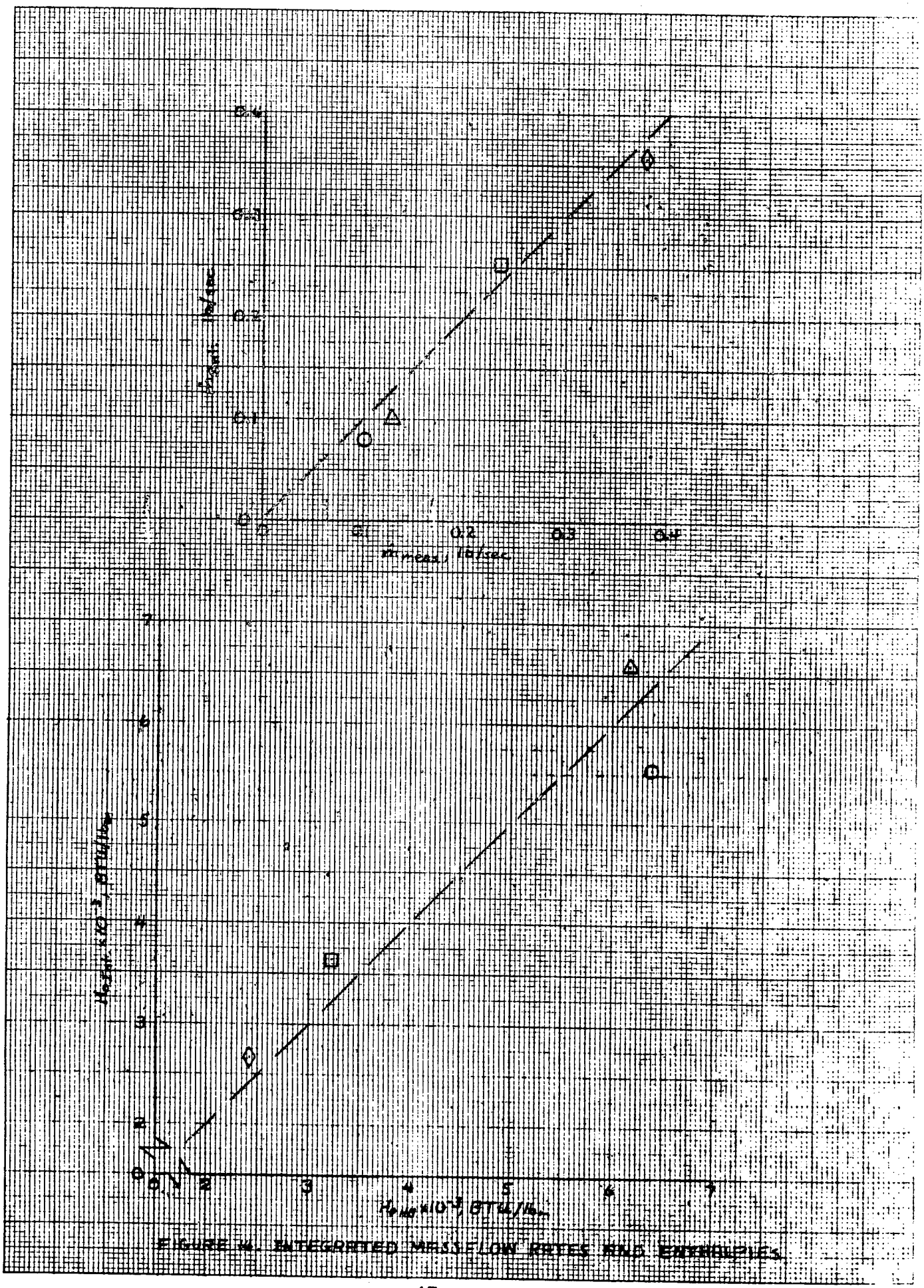

FIGURE 14. INTEGRATED MASS FLOW RATES AND ENTHALPIES.

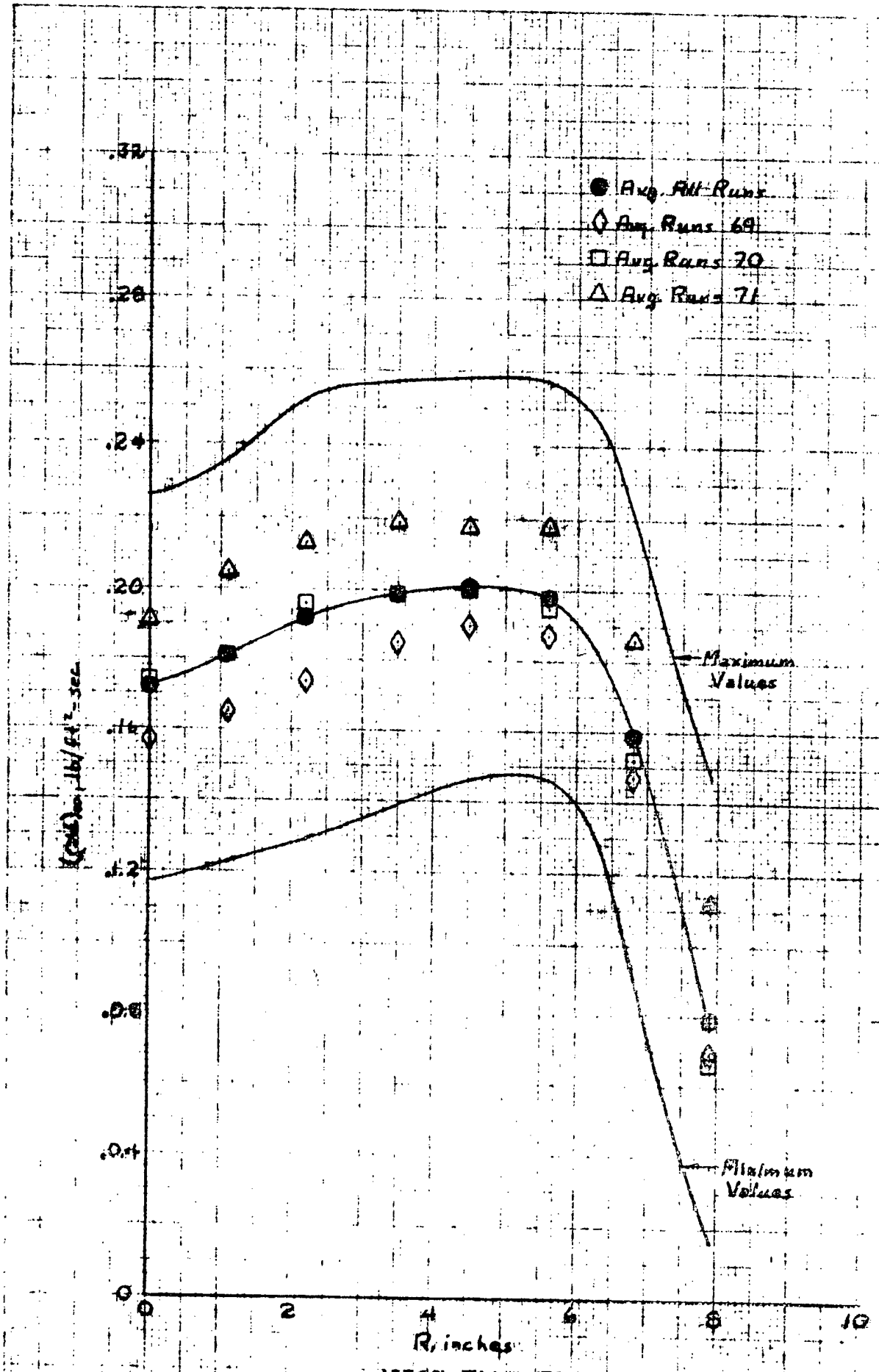

a. MASS FLUX PROFILE

FIGURE 15. AVERAGE TEST SECTION MEASUREMENTS FOR D_{HE} = 19.36 IN., R_e = 350

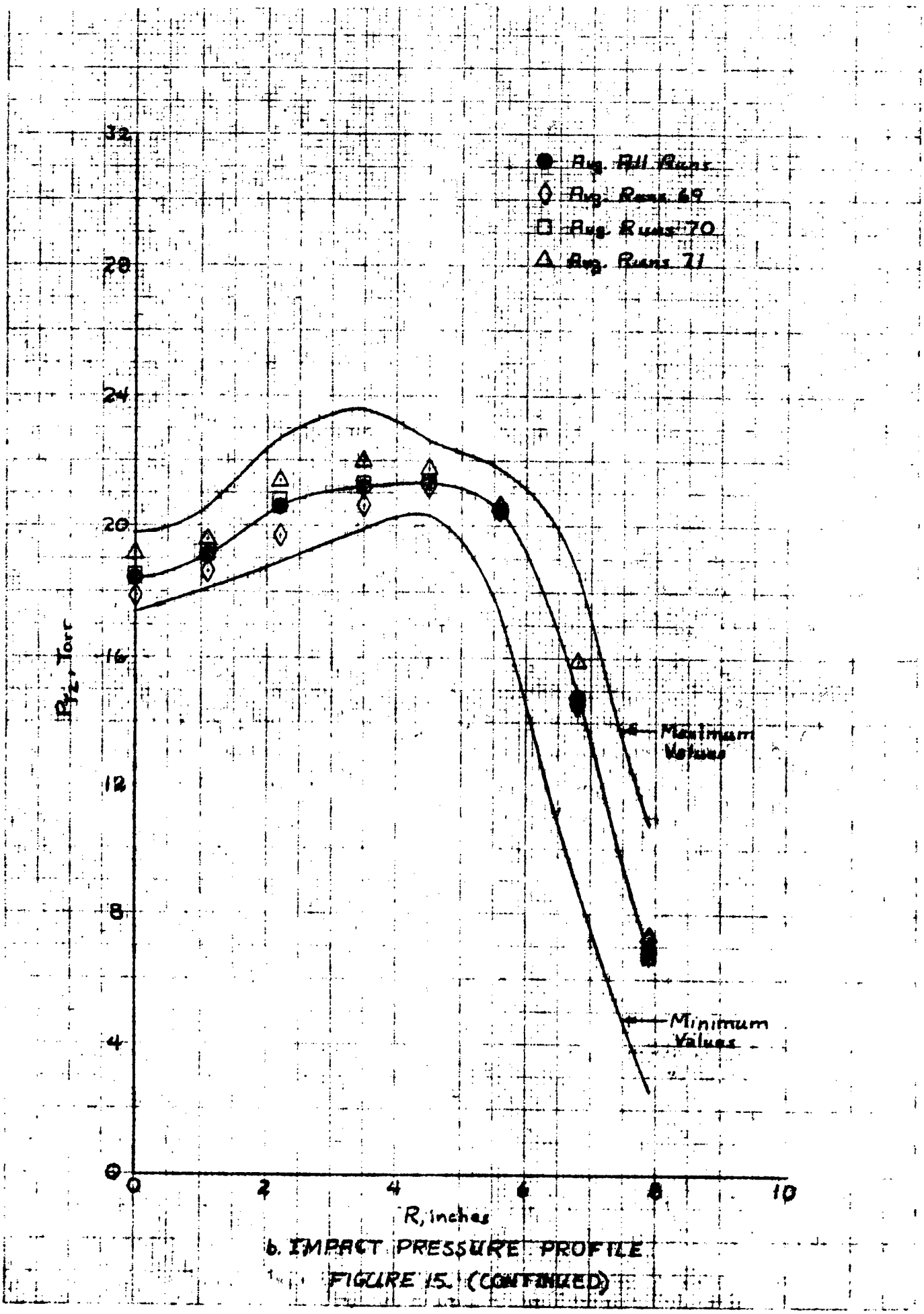

b. IMPACT PRESSURE PROFILE.

FIGURE 15. (CONTINUED)

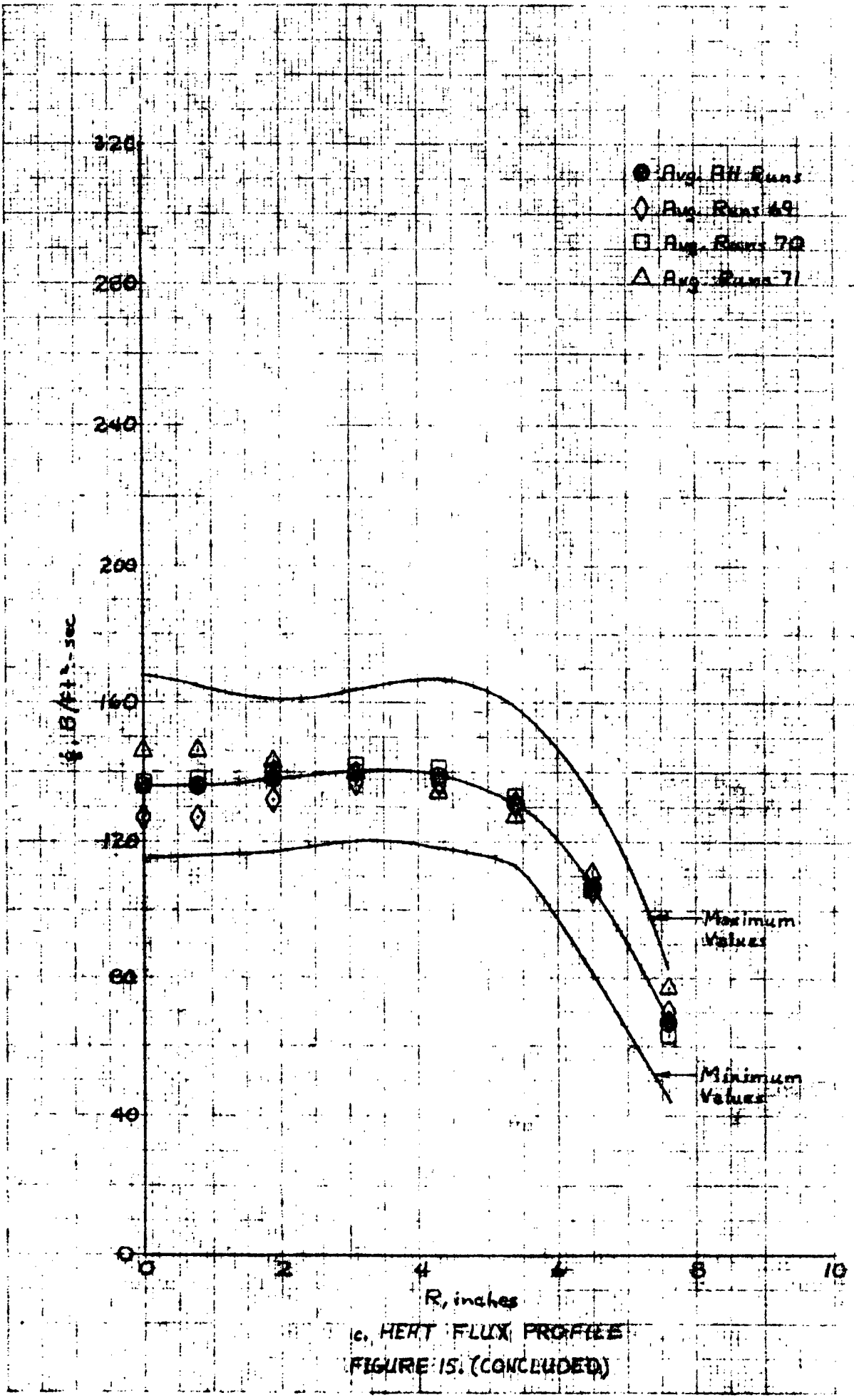

c. HEAT FLUX PROFILE

FIGURE 15. (CONCLUDED)